FORUM REVIEW ARTICLE

Signaling and regulation through the NAD^+ and $NADP^+$ networks

By
Ilmo E. Hassinen
Faculty of Biochemistry and Molecular Medicine
University of Oulu, Finland

Running head: Regulation through NAD(P) network

Keywords: Redox state, redox regulation, energy metabolism, transmembrane carrier, NAD^+ and $NADP^+$-dependent protein modification

Address correspondence to:
Ilmo E. Hassinen, M.D., Ph.D.
Faculty of Biochemistry and Molecular Medicine
P.O. Box 5400
FI-90014 UNIVERSITY OF OULU
FINLAND
Courier address:
Aapistie 7 A
FI-90220 Oulu,
FINLAND
e-mail: ilmo.hassinen@oulu.fi
phone: +358 294485802
mobile: +358 50 3585502

Word count 8000 (w/o refs, figure legends and abbreviation list), 173 references, 6 gray tone figures, no color figures.

Abstract:

Significance: NAD^+ and $NADP^+$ are important co-substrates in redox reactions and participate in regulatory networks operating in adjustment of metabolic pathways. Moreover, NAD^+ is a co-substrate in post-translational modification of proteins and is involved in DNA repair. NADPH is indispensable for reductive syntheses and the redox chemistry involved in attaining and maintaining correct protein conformation.

Recent Advances: Within a pair of decades, a wealth of information has been gathered on $NAD(H)^+$/NADP(H) redox imaging, regulatory role of redox potential in assembly of spatial protein structures and the role of ADP-ribosylation of regulatory proteins affecting both gene expression and metabolism. All this as a bearing also on disease, healthy ageing and longevity.

Critical Issues: Knowledge of the signal propagation paths of NAD^+-dependent post-translational modifications is still fragmentary for explaining the mechanism of cellular stress effects and nutritional state on these actions. Evaluation of the co-substrate and regulator roles of NAD(H) and NADP(H) still suffers from some controversies in experimental data.

Future Directions: Activating or inhibiting interventions in NAD^+-dependent protein modifications for medical purposes have shown promise, but restraining tumor growth by inhibiting DNA repair in tumors by means of interference in sirtuins is still in early stage. The same is true for the use of this technology in improving health and healthy ageing. New methods for monitoring the nicotinamide-adenine nucleotides in intact cells and organs are developed, and their application to medicine is expected.

Introduction

The early work of Theodor Bücher and Martin Klingenberg delineated the concept of redox networks in living organisms (12).

The redox-dependent nucleotide-consuming or -producing signal pathways, the availability of reduced glutathione and maintenance of cysteine and disulfide bridges in proteins are another mainline of redox research. Helmut Sies and coworkers have coined the concept "redox code" to emphasize the role of redox co-substrates in metabolic regulation (74). Intercompartmental differences in the steady-state redox potentials exist (77,137), although near-equilibrium states participate in signaling and regulation under certain conditions (164).

The most efficient biological energy conversion system captures the combustion energy of oxygen reduction by the mitochondrial respiratory chain, fueled by reducing equivalents from energy metabolism. Redox-dependent control is positioned to reactions where the substrate or co-substrate concentration is low compared with the K_m of the enzyme. Even a near-equilibrium of an NAD(H)- or NADP(H)-linked enzyme reaction may perform as a regulator of an adjunct enzyme, when the concentration of a metabolic intermediate is poised by the ratio of the oxidized and reduced form of the coenzyme, leading to redox-governed substrate control of the enzyme reaction (Fig. 1). The redox ratios of hydride-transferring nucleotides are also involved in feedback regulation of metabolic pathways by allosteric interactions.

After increasing appreciation of the significance of nitrogen- and oxygen-containing reactive oxidative species, the scope of redox biology includes also oxidative stress (137). However, in the present treatise, the reactive oxygen and nitrogen species are left out because of lack of space.

Interplay between mitochondrial and cytosolic redox organizations

The mitochondrial electron transport chain (ETC) builds a pH gradient and membrane potential across the inner mitochondrial membrane (MIM). Together they constitute the electrochemical potential of protons ($\Delta\mu\tilde{}H^+$), which is conserved in ATP by the F_1F_o-ATP synthase (for a review, see (85)).

It is assumed that the free NADH concentration in the mitochondrial matrix is much above 2 µM, which is the apparent K_m^{NADH} of NADH:ubiquinone oxidoreductase (Complex I) in submitochondrial particles from bovine heart (155). Thus, mitochondrial respiration is normally not regulated simply by NADH availability but the redox potential of the matrix NADH/NAD^+ couple, because it defines the free energy change in the reduction of oxygen to water, the driving force of the ETC (164). The last reaction, catalyzed by cytochrome *c* oxidase (Complex IV) is controlled by several modes of enzyme regulation but obeys the rules of irreversible thermodynamics (158) that predict that oxygen reduction by the respiratory chain is proportional to the driving force determined by the redox potential difference between NADH/NAD^+ and oxygen. However, there are near-equilibrium conditions between the ATP synthase and at the two proximal energy conversion sites of ETC that influence the redox potentials of the electron carriers including cytochrome *c*, the substrate of Complex IV. Thus, cell respiration becomes determined by the energy status of the cell (53,54,77,93,162,164).

The mammalian MIM, which is impervious to NADH or NAD^+, exploits $\Delta\tilde{\mu}H^+$ also to build a redox potential difference between NADH/NAD^+ pools of cytosol and mitochondria. This difference (mitochondrial matrix more negative) in an isolated perfused rat heart approaches the magnitude of the mitochondrial membrane potential (77). The cytosolic NAD(H) redox potential in rat heart muscle is -215 mV, which corresponds to free NADH/NAD^+ ratio around 0.0001, and the mitochondrial matrix redox potential of -314 mV corresponds to a free NADH/NAD^+ ratio of 0.143. The situation is similar in the isolated perfused liver (142) . The low proportion of free NADH is a dilemma for absorption spectrophotometric monitoring of free cytosolic NADH, because its

concentration changes are too small to be accurately detectable by in intact tissues, where the bound fraction dominates (11).

The mitochondrial solute carrier family 25 (SLC25) contains 53 structurally homologous members (33,69). Although a variety of purine and pyrimidine nucleotides are translocated by them, the nicotinamide nucleotides are not (81,151). Because of the impermeability of MIM to NAD(H) and NADP(H), the cells are forced to resort to substrate shuttles involving NAD^+ or $NADP^+$-linked enzymes and metabolite exchange translocators.

Malate-aspartate shuttle

It is remarkable that transfer of reducing equivalents to mitochondria occurs against a thermodynamic gradient, because the mitochondrial free NADH/NAD^+ ratio is higher than the cytosolic one (Fig. 2). The redox gradient is retained by coupling an electrogenic NAD^+-linked metabolite translocation shuttle to $\Delta\tilde{\mu}H^+$ across MIM. The shuttle employs cytosolic and mitochondrial malate dehydrogenases and cytosolic and mitochondrial aspartate aminotransferases (to circumvent oxaloacetate impermeability of MIM), and the glutamate/aspartate and 2-oxoglutarate/malate exchange translocators. The glutamate/aspartate carrier is driven by $\Delta\tilde{\mu}H^+$ because it transports aspartate as an anion and glutamate together with a proton. As described above, the redox potential difference between the cytosolic and mitochondrial NADH/NAD^+ couples is comparable to the membrane potential as confirmed with the indicator enzyme approach and non-aqueous tissue fractionation in heart muscle (77). In excitable cells the glutamate/aspartate translocator has calcium-binding isomorphs making the shuttle calcium-activated (119).

The animal mitochondrial MIM lacks an NADH/NAD^+ translocator with reason, because transgenic human cells expressing *Arabidopsis* mitochondrial NAD^+ translocator are unable to perform oxidative phosphorylation and revert to glycolytic energy supply (151). Evidently the redox potential difference between mitochondrial and cytosolic NAD(H) couples is indispensable. One explanation could be that an NADH/NAD^+ translocator in combination with the electrogenic malate-aspartate shuttle discharges $\Delta\mu\tilde{}H^+$. The electrogenic malate-aspartate shuttle apparently has the additional duty to keep the mitochondrial NADH/NAD^+ couple sufficiently reduced to provide sufficient free energy change across complex I to allow its conventional proton pumping stoichiometry of 4 $H^+/2e^-$. The true pumping stoichiometry of Complex I is still under some debate, because it is limited by the redox potential difference between the NAD(H) and ubiquinone (73,159).

Glycerophosphate shuttle

Another possibility to reoxidize cytosolic NADH is the glycerophosphate shuttle driven by the cytosolic NAD^+-linked glycerol-3-phosphate dehydrogenase and the MIM flavoenzyme glycerol-3-phosphate:ubiquinone oxidoreductase (mtGPDH) belonging to the membrane-bound, flavin-containing dehydrogenases (23). The glycerophosphate-interacting site of mtGPDH faces the mitochondrial intermembrane space, so that the substrate has no need to enter the mitochondrial matrix (80). In most mammalian tissues (liver, kidney, heart) mtGPDH activity is rather low, but is enhanced by the thyroid hormone (88). High glycerophosphate oxidation rates are found in the β-cells of the Langerhans isles (135) and brown fat cells (133). The activity is extremely high in insect flight muscle (26). A shortcoming of the glycerophosphate shuttle is that it bypasses the first energy conserving site of the ETC.

MtGPDH produces reactive oxygen species (ROS), but the source of ROS during glycerophosphate oxidation is not the mtGPDH flavin but the ubiquinone-binding site, where semiubiquinone probably leaks reducing equivalents to oxygen (109,117).

The NAD-linked metabolic and regulatory grid

The steady-state free NADH/NAD^+ ratio is determined by the production and utilization of reducing equivalents. In glycolysis the dehydrogenation reactions are dependent on a continual source of NAD^+ as a hydride acceptor. Under conditions where NADH reoxidation mechanisms are limiting, pyruvate is used as an oxidant in the lactate dehydrogenase (LDH) reaction. Lactate represents a metabolic dead end and must be exported. LDH activity in most cells is sufficient to attain near-equilibrium, so that the [lactate]/[pyruvate] ratio in cytosol reflects the free NADH/NAD^+ ratio. In aerobiosis, pyruvate enters the mitochondria through the monocarboxylate translocator or a specific pyruvate translocator (for a review, see (145)).

The redox potential of the NAD(H) couple participates in regulation of metabolism at several levels (Fig. 3). These redox-active coenzymes may act as allosteric inhibitors, activators, or product inhibitors. The redox balance is able to control metabolic flux also if the concentration of an intermediate falls near or below the K_m of the metabolizing enzyme.

Regulation of pyruvate metabolism

Pyruvate dehydrogenase complex (PDC) catalyzes an irreversible oxidative decarboxylation to produce acetyl-CoA, CO_2 and NADH. It is comprised of three collaborating enzymes: pyruvate dehydrogenase (PDH; E1), dihydrolipoamide acetyltransferase (E2) and dihydrolipoamide dehydrogenase (E3), which is an FAD-containing flavoenzyme. The size of PDC is enormous: 30 $\alpha_2\beta_2$ heterotetramers of E1 and six E3 dimers bind to a 60-meric E2/E3BP (E3-binding protein) core (44).

The PDC co-substrates NAD^+ and CoA-SH participate also in regulation of the enzyme by acting as effectors of four isomorphs of PDH-inactivating protein kinase (PDK1-4) and two isomorphs of PDH-activating protein phosphatase (PDP1-2) that show organ-specific expression patterns (62). The phosphorylation occurs into three E1serine residues (62). This covalent protein modification mode of regulation provides amplification, because even a small difference between the reciprocal kinase and phosphatase activities results in extensive change in the PDH capacity.

The PDC kinases are activated by NADH and acetyl-CoA and inhibited by pyruvate. This, in effect makes PDC regulated by the NADH/NAD^+ and acetyl-CoA/CoA-SH ratios. Of the PDC phosphate phosphatases, PDP1 is activated by Mg^{2+} and PDP2 by Ca^{2+} (106). Because mitochondrial matrix Mg^{2+} is partly chelated by ATP, the free Mg^{2+} decreases when ATP concentration increases (43,90), so that PDC becomes inhibited upon ATP increase and activated by free Ca^{2+} increase. To summarize, the covalent interconversions of PDH become regulated by the redox potential of the NADH/NAD^+ couple, the acetyl-CoA/CoA-SH ratio and the cellular 'phosphorylation potential' ([ATP]/{[ADP]·[Pi]} ratio). This is feasible because acetyl-CoA, the product of the PDH reaction, is the fuel of the TCA cycle, which is largely regulated by the cellular ATP consumption and the NADH/NAD^+ couple.

NADH regulation of the tricarboxylic acid cycle

Several TCA cycle enzymes are subjected to redox- or energy-linked regulation. Citrate synthase is fed with a co-substrate whose concentration is connected to the mitochondrial NAD^+/NADH ratio, and due to its regulatory characteristics the NAD-linked isocitrate dehydrogenase (IDH3) is a central pacemaker of TCA cycle. IDH3 is inhibited by NADH, NADPH and ATP and activated by Ca^{2+} and Mg^{2+} (100,122). Also Mg^{2+} links regulation to the cellular energy state, because ATP is a chelator of Mg^{2+}, so that a decrease of ATP increases the free concentration of Mg^{2+} (43,90). The situation mimics Mg^{2+} activation of pyruvate dehydrogenase phosphatase, which leads to conversion of PDH to its active state upon cell de-energization.

The next TCA cycle enzyme, 2-oxoglutarate dehydrogenase (OGDH) is also effectively regulated by redox potential and energy state. It is inhibited by increases in the NADH/NAD^+ and ATP/ADP ratios (29). The subunit and coenzyme composition of OGDH is homologous of PDH, although the former is not regulated by covalent interconversions. The lipoamide dehydrogenase subunit of OGDH links it to the cellular redox balance of the S-S/SH ratio in proteins. The dihydrolipoyl dehydrogenase component of OGDH is an NAD^+-linked, FAD-containing enzyme and displays flavin fluorescence applicable to compartment-specific monitoring of the free NADH/NAD^+ ratio in mitochondrial matrix.

Non-decarboxylating (NAD-linked) and decarboxylating (NADP-linked) malate dehydrogenases

NAD^+ and $NADP^+$-linked malate dehydrogenases exist in mitochondria and cytosol. The NAD^+-linked form (ME2) participates in the TCA cycle. The pyruvate-producing, $NADP^+$-linked, decarboxylating malate dehydrogenase ("malic enzyme") exists as cytosolic (ME1) and mitochondrial (ME3) isoenzyme and participates in the regulation of total TCA cycle metabolite pool by means of anaplerosis and cataplerosis. Under average conditions the reaction runs in the direction of pyruvate carboxylation and anaplerosis, but the flux reverses under conditions of excessive influx of substrates to the TCA cycle, and the enzyme operates as a decarboxylating dehydrogenase (144). The NADP-linked malic enzyme has been suggested to be involved also in insulin secretion by the pancreatic β-cells, although the literature is controversial (49). Majority of the malic enzyme is located in the cytosol (in human liver 90% extramitochondrial), where it is one of the sources of reducing power in the form of NADPH needed for biosynthetic pathways such as fatty acid synthesis (169).

An extreme example of spreading metabolic redox imbalance: situation during ethanol oxidation in liver

An extreme case of metabolic regulation by redox organization is exemplified by ethanol oxidation in liver, where its oxidation to acetate produces large amounts NADH, which by mediation of the redox substrate shuttles increases also the mitochondrial NADH/NAD^+ ratio. Under these conditions, pyruvate concentration decreases both in cytosol and mitochondria, so that the gluconeogenic pyruvate carboxylation reaction becomes restricted by substrate limitation (83). Also the redox poise of other NAD^+-linked dehydrogenation reactions in near-equilibrium shifts towards accumulation of reduced metabolites. NADH accumulation drives the malate dehydrogenase reaction towards malate accumulation and oxaloacetate depletion. The normal free oxaloacetate concentration is around the K_m of citrate synthase (140), so that citrate synthase is oxaloacetate-limited i.e. rate-limiting for the TCA cycle (for references see (161)). Therefore, during active ethanol oxidation TCA cycle in liver becomes halted, as indicated by stopping of CO_2 production in spite of normal oxygen consumption (36).

The control of the TCA cycle is distributed: NADH is an allosteric inhibitor of citrate synthase, and the cycle flux is regulated by the mitochondrial NAD^+-linked isocitrate dehydrogenase (IDH3), which is controlled by the NADH/NAD^+ ratio. In cardiac muscle the control strength of IDH3 appears equal to that of citrate synthase, as demonstrated by an increase of citrate and isocitrate and decrease in 2-oxoglutarate concentration upon decrease in ATP consumption (59).

The excessive cytosolic NADH production during ethanol metabolism in liver has a bearing even on lipid metabolism by increasing the [glycerol-3-phosphate]/[dihydroxyacetone phosphate] ratio. Glycerol-3-phosphate (G3P) is a precursor of triacylglycerol synthesis, which also increases. Although there is a linear correlation between hepatic G3P concentration and the activity of

phosphatidate phosphatase (PAP), a regulatory enzyme of triacylglycerol synthesis (130), the development of acute ethanolic fatty liver is more complicated, because PAP expression and activity are under strong hormonal control (82,89).

This ethanol-exerted rechanneling of energy metabolism emphasizes the power of redox organization in control of the TCA cycle. The ethanol-induced halt of hepatic TCA cycle and gluconeogenesis in liver exemplifies a situation where cell respiration becomes dominated by oxidation of reduced equivalents without TCA cycle contribution. It has been proposed that this is the principal sequence of developing alcoholic hypoglycemia under conditions of low hepatic glycogen stores (83).

NADP(H) as a co-substrate and regulator

$NADP^+$-linked redox regulation

NADPH is required in reductive syntheses and also in regulation and maintenance of the redox-active thiol/disulfide balance and is an electron donor in production of ROS for immune defense and signaling (120). In the context of redox chemistry of proteins, availability of reduced glutathione (GSH) is essential. It reacts with protein disulfide groups in a reaction which converts it to glutathione disulfide (GSSG). The latter is reduced to GSH by the FAD-linked glutathione reductase enzyme at the expense of NADPH (25). Glutathione is used as reducing power for reducing glutaredoxins. The reduced glutaredoxins then reduce the target proteins. Reduced glutaredoxin is regenerated in a non-enzymatic reaction with GSH (94).

Proton-translocating transhydrogenase

MIM contains an energy-linked, proton-pumping NADH-$NADP^+$ transhydrogenase, which catalyzes mitochondrial matrix $NADP^+$ reduction with NADH by employing the $\Delta\mu\tilde{}H^+$ as an energy source. As a consequence, the equilibrium of transhydrogenation shifts from unity to 500 in favor of NADPH formation in the presence of a $\Delta\mu\tilde{}H^+$, so that the mitochondrial $NADP^+$ is typically about 95% reduced (8), i.e. much more reduced than NAD^+ which is only 14% reduced in mitochondria of an isolated perfused rat heart (77,114). The mitochondrial NAD^+ concentration is considered to be several times higher than the cytosolic one (15,32), although published data from direct determination are scarce.

$NADP^+$-linked substrate cycles for transmembrane transport of reducing equivalents

The steady-state redox potential of the NADPH/$NADP^+$ couple (similarly to NADH/NAD^+) is heavily compartmentalized. In the mitochondrial matrix, $NADP^+$ is, similarly to NAD^+, much more reduced than in the cytosol because of the proton-pumping NAD-NADP transhydrogenase, which employs the $\Delta\mu\tilde{}H^+$ across MIM for reducing $NADP^+$ by employing the NADH/NAD^+ couple as a driving force. The transhydrogenase reaction is reversible so that under conditions of high NADH/NAD^+ ratio and low proton motive force the transhydrogenase is able to pump out protons from the mitochondrial matrix.

The extremely high reducing power of the mitochondrial NADPH/$NADP^+$ couple is made available also in cytosol to cover the requirements of reductive syntheses. Because no $NADP^+$ or NADPH translocators exist in MIM, transfer of reducing equivalents occurs by substrate cycles.

In the cytosol, the conventional major NADPH source is the pentose phosphate pathway (PPP), but cytosolic $NADP^+$ can be reduced also from mitochondrial sources. To this effect, mitochondrial

2-oxoglutarate is reduced by reversal of the $NADP^+$-linked isocitrate dehydrogenase (IDH2) reaction so that reducing equivalents are saved as isocitrate, which after isomerization to citrate by aconitase is exported to cytosol, where it is back-isomerized by aconitase and oxidized by the cytosolic $NADP^+$-linked isocitrate dehydrogenase isoform IDH1 to regenerate NADPH. This citrate shuttle plays a dual role: It transfers of both acetyl-CoA and reducing power from mitochondria for cytosolic fatty acid synthesis. The former is accomplished by ATP-citrate lyase and the latter by IDH1 (Fig. 1).

The mitochondrial (ME3) and cytosolic (ME1) isoforms of malic enzyme may also function as an NADP-linked conveyor of reducing equivalents from mitochondria to cytosol via the dicarboxylate carrier. The coordinated traffic of reducing power and carbon as malate and citrate via the dicarboxylate and tricarboxylate carriers comprises an entity called 'citrate-malate shuttle'.

Pentose Phosphate Pathway

In addition to glycolysis, glucose-6-phosphate can take an alternative, markedly different oxidative route, namely, the pentose phosphate pathway (PPP), which provides ribose precursors for nucleotide synthesis and reducing power in the form of NADPH. It also participates in the regulation of cellular growth and protection against oxidative damage. The first committed step of PPP is catalyzed by the $NADP^+$-linked glucose-6-phosphate dehydrogenase (G6PDH). The product 6-phosphogluconolactone is hydrolyzed by means of the 6-phosphogluconolactonase to 6-phosphogluconate, which produces NADPH in the 6-phosphogluconate dehydrogenase reaction. In addition to this oxidative branch, PPP can be visualized to have a non-oxidative branch, which metabolizes pentose, tetrose, and triose phosphate intermediates back to glucose-6-phosphate in order to enable complete oxidation of glucose-6-phosphate in PPP (for description, see (84)).

G6PDH is the rate-limiting and regulatory enzyme of PPP. According to the conventional view, G6PDH activity is regulated by transcriptional control in parallel with other lipogenic enzymes. However, the regulation involves a multitude of mechanisms: both rapid metabolic and slower transcriptional and post-transcriptional events. E.g. after initiation of a "respiratory burst" (147) in phagocytes the first metabolic effect is inhibition of glycolysis to spare glucose for PPP. Eggleston and Krebs (35) emphasized that the activation of PPP must rather be regarded as de-inhibition, because the basal NADPH concentration is several orders of magnitude higher than the K_i^{NADPH} of G6PDH (17) so that the enzyme is almost completely inhibited.

The inhibition by NADPH can be released by GSSG, and a thiol exchanger protein has been isolated (127). This means that its glutathionylation is involved in the regulation of G6PDH. Protein-protein interactions appear to be involved in the rapid de-inhibition, and according to another proposal, the proteins are considered to trap NADPH in a rapid reaction to alleviate inhibition and to activate G6PDH (112,123).

It is evident that defects of the non-oxidative part of PPP affect also the flux through the two NADPH-yielding steps in its oxidative branch. Maintaining of GSH redox status has a bearing even on the integrity of mitochondria as indicated by the functional defects of mitochondria caused by transaldolase deficiency resulting in reduction of mitochondrial mass and membrane potential (121).

Maintenance of the size of compartmental $NAD(P)^+$ pools

Mitochondria

The mitochondrial outer membrane (MOM) is freely permeable to most small molecular weight compounds through pore formations. MIM is impermeable to NAD(H) and NADP(H), which have to be synthesized within the mitochondria, and the precursors must be transported across MIM or

recycled by other means (Fig. 4). Two modes of NAD^+ synthesis exist: the *de novo* synthesis, which starts from tryptophan and uses the kynurenine pathway, or the *salvage* pathways, which use nicotinamide (Nam), nicotinamide riboside (NamR) or nicotinamide mononucleotide (NMN) as precursors. NamR cannot be a precursor of mitochondrial NAD synthesis, because both known isoforms of NamR kinase (NRK1 and NRK2) are located in the cytosol or nucleoplasm (111). It is remarkable that NMN is metabolized extracellularly to NR, which is then taken up by the cells and converted into NAD^+ even in NRK1-KO animals (124). Because thymidylate kinase 2 (TK2) is homologous to NRK and has a mitochondrial isoform, TK2 could be capable of NamR phosphorylation, but TK2 overexpression experiments demonstrate that it is not involved in mitochondrial NAD^+ synthesis (111). Thus, all the currently available data suggest that NMN is the main precursor in the mitochondrion, although a responsible translocator for it has not been identified (for references, see (141)). NMN in mitochondria is converted to NAD^+ by the mitochondrial isomorph of nicotinamide mononucleotide adenylyl transferases (NMNAT) by using ATP as the adenylyl source (for references, see. (141)).

The size of the mitochondrial $NADH^+/NAD^+$ pool is adjusted by the rates of *de novo* synthesis and degradation in mitochondria. The NAD^+-consuming enzymes in mitochondria include families of *Diphtheria* toxin-related ADP-ribosyltransferases (ARTs) including poly-ADP-ribosyl-polymerases (PARP) and mono-ADP-ribose transferases which link ADP-ribose moieties to various acceptors proteins including sirtuins.

The mitochondrial $NADP^+$ pool is maintained by NADK2, the recently found mitochondrial isoform of NAD kinase (115,171). Its human mutation leads to deficiencies of mitochondrial NADP and the NADP-linked 2,4-dienoyl-CoA reductase (DECR) activity and results also in hyperlysinemia (65).

Peroxisomes

Peroxisomes are single-membrane organelles with a selection of oxidative enzymes, which do not directly conserve combustion energy by complete reduction of oxygen, but are essential for oxidation of certain amphipathic molecules. For complete oxidation, long- and very-long-chain fatty acid-CoAs are first chain-shortened in peroxisomes in a β-oxidation process yielding NADH and H_2O_2 and then transferred to mitochondria for complete oxidation (Fig. 5). This collaboration of peroxisomes with mitochondria during long-chain fatty acid oxidation can be demonstrated by optical monitoring of changes in NAD(P)H and catalase-H_2O_2 complex concentration, which is dependent on hydrogen peroxide production rate. This enzyme substrate complex was originally identified in purified catalase by Britton Chance in 1947 and named Compound I (18,19). Subsequently the concentration of the H_2O_2-catalase complex has been employed as a hydrogen peroxide production probe in intact perfused liver by means of organ spectrophotometry to evaluate peroxisome-dependent oxidations (20,50,60,76,118,138).

Even biogenesis of peroxisomes is dependent on mitochondria. Peroxisome maturation necessitates peroxins to import of proteins into the peroxisomal matrix. In the absence of pre-peroxisomes the peroxins are mistargeted into MOM (Fig.5) (143). *De novo* pre-peroxisomes originating from ER amalgamate subsequently with mitochondrion-derived vesicles to acquire membrane lipids and peroxins, which allow import of proteinaceous components to the maturating peroxisomes (for a review, see (37)).

NAD^+ is essential for the peroxisomal fatty acid oxidation, but in contrast to mitochondria, peroxisomes are not capable of *de novo* synthesis of NAD^+ (Fig. 6). However, peroxisomes are able to replenish or grow their NAD^+ pool size by means of the SLC25A17 translocator (2) by an exchange mechanism, or the degradation products can leave the organelle through the PXMP2 channels (4,5,128). Diminution of the peroxisomal NAD(H) pool must be carried out by

decomposition of NAD^+ or NADH by the NUDT12 hydrolase of the Nudix family of pyrophosphatases (1). Plant peroxisomes contain also PXN, an NAD^+ translocator, which is capable to transport NAD^+ in exchange for AMP but not for NADH, indicating that PXN is not able to function as a NADH/NAD^+ exchanger (150). Depending on species, the peroxisomes contain LDH, glycerol-3-phosphate dehydrogenase (G3PDH) and malate dehydrogenase, so that lactate/pyruvate, glycerol-3-phosphate (G3P)/dioxyacetone phosphate (DOAP), and malate/oxaloacetate shuttles are possible (150). Etherphospholipid synthesis in peroxisomes consumes DOAP or G3P that is another requirement for G3PDH and a channel (PXPM2) permeable to DOAP and G3P (for a review, see (157)). The NADPH-requiring acyl-CoA reductase enzyme of the etherphospholipid synthesis pathway is located on the outer surface of peroxisome, so that an $NADP^+$-linked shuttle or channel is unnecessary (63). In vertebrates, extended forms MDH1x and LDHBx of MDH1 and LDHB, respectively, are produced by translational read-through extension and contain C-terminal peroxisomal import sequences and are directed to peroxisomes (61,134).

NADPH is indispensable for oxidation of unsaturated fatty acids, because the dienoyl configuration is energetically unfavorable for β-oxidation and has to be removed by the NADPH-linked 2,4-dienoyl-CoA reductase (60,67). $NADP^+$ is produced by the NAD^+ kinase (NADK), but only a cytosolic NADK1 and a mitochondrial NADK2 isoform have been identified in animals (115,171), although *Arabidopsis thaliana* possesses two NAD kinase isomorphs (NADK1 and NADK2) and a third, which preferentially phosphorylates NADH, is peroxisomal and named NADK3 (156). In animals, a peroxisomal NADK remains to be discovered. Depending on the phylum, NADK is regulated by direct activation by a Ca^{2+}/calmodulin or phosphorylation by a Ca^{2+}/calmodulin dependent kinase (96).

One-carbon pathway in NADP pool maintenance

Recently, the function of the one-carbon (serine, folate, and glycine) pathway in supplying mitochondrial NADPH has been increasingly appreciated. The one-carbon pathway is upregulated at the gene expression level in tumors (146), as expected on the basis of the finding that cancer cell proliferation is dependent on serine and one-carbon pathway, which is involved in the production of nucleotides including ATP and $NADP^+$ (110). The one-carbon pathway, which operates both in the cytosol and mitochondria, consumes NADH and produces NADP so that changes in the cellular redox organization in cancer cells are anticipated (22), and such has been observed in precancerous cells (152).

NADPH/$NADP^+$ ratio, thiol/disulfide balance and protein folding,

For proteins directed towards secretion, the post-translational folding for attaining their native 3D structure occurs in endoplasmic reticulum (ER). The folding process is closely linked to redox potential, because it is dependent on thiol/disulfide balance. This means that ER must possess thiol conserving and oxidizing tools. The reducing processes necessitate cytosolic glutathione synthesis, which is dependent on NADPH. Disulfide bridges are produced by oxidative mechanisms provided by a thiol/disulfide exchange enzyme named protein disulfide isomerase (PDI) and luminal thiol oxidase ERO1, an H_2O_2 producing flavoenzyme, which functions as a conveyor of electrons from PDI (for a review, see (55)). Also peroxiredoxin 4 (PRDX4), which is located in ER, produces disulfide bonds by using H_2O_2 as an oxidant, although the source of H_2O_2 remains to be identified (105).

Energy state detectors in cells

The cellular energy currency is ATP, but the stores are not determined only by ATP concentration but the free energy of its hydrolysis to ADP and inorganic phosphate (P_i). The best indicator would be the mass-action ratio [ATP]/{[ADP]·[P_i]} (also called 'phosphate potential'), taken from the Gibbs equation $\Delta G = \Delta G^o + RT \cdot ln\{([ADP] \cdot [P_i])/[ATP]\}$, where ΔG and ΔG^o are actual and standard free energy change, respectively, R is the gas constant and T is the temperature in Kelvins.

The "energy charge", ([ATP]+[½ADP])/([ATP]+[ADP]+[AMP]) is a rough estimate of the cellular energy state (6), although its relation to free energy change is not linear. As emphasized above, the adenylate kinase reaction, 2 ADP ↔ AMP + ATP, makes AMP concentration to a sensitive energy state indicator, because it is proportional to the square of ADP concentration. Moreover, because ATP is an inhibitor of AMPK, the latter becomes a probe of AMP/ATP ratio (75).

NAD^+-consuming signaling

The data described above are the basis of linking more structural or genomic variables to the cellular oxidation-reduction organization. Although NAD^+ belongs to the metabolic coenzymes participating in hydride transfer and even functions as a messenger, it serves as a substrate for reactions, which modify or produce regulator molecules. In this capacity NAD^+ is a sensor of the metabolic situation.

ADP-ribosyltransferases and sirtuins

The NAD^+-consuming enzymes comprise families of ADP-ribosyltransferases (ART) including poly-ADP-ribosyl-polymerases (PARP), mono-ADP-ribose transferases which link ADP-ribose moieties of various acceptors such as proteins, and sirtuins (64). Sirtuins are a homologs of the silent information regulator 2 (SIR2), an epigenetic gene silencing regulator in yeast, acting by protein deacetylation and deacylation using NAD^+ as an energy source. Histone acetylation slackens the nucleosome, increasing the accessibility of the DNA to expression modifiers, whereas deacetylation results in gene silencing (172). However, when the target is a non-histone protein, the direction of the effect of deacetylation is variable: SIRT3 deacetylates and activates e.g. glutamate dehydrogenase, isocitrate dehydrogenase 2 (131) and mitochondrial acetyl-CoA synthetase (AceCS2) (47). Only SIRT1 deacetylates and activates the cytosolic AceCS1. Also the peroxisome proliferator-activated receptor-γ coactivator-1a (PGC-1α), which is a regulator of gluconeogenesis and fatty acid oxidation in liver, is deacetylated and activated by SIRT1 (71,126).

The relation between SIRT1 and the tumor suppressor protein p53 is different: SIRT1 was initially considered to be a tumor promotor by repressing p53, but later it was found that SIRT1 affects the intracellular location of p53. Deacetylation prevents p53 passage into the nucleus, so that it translocates into mitochondria, where it activates transcription-independent, apoptosis, which ultimately has a tumor-suppressing effect (for a review, see (42)).

Although the NAD^+-consuming capacity of sirtuins is less than that of the ART/PARP class of enzymes, they are in the focus of current research because of their involvement in cell survival, longevity and metabolic regulation. As regulators, the sirtuins control a wide metabolic network in response to nutritional situations (Fig. 4). Their activity is linked e.g. to glucose homeostasis at the level of hepatic gluconeogenesis, pancreatic insulin secretion and peripheral insulin sensitivity that is at least partly mediated by (PGC-1α) (126) and is associated with metabolic syndrome and type II diabetes.

Sirtuins are linked to energy-linked metabolic regulation and energy deficit through to the AMP-dependent protein kinase (AMPK) activity. It has been demonstrated that AMPK activators decrease the acetylation grade of PGC-1α in glycolytic but not oxidative aerobic muscle (14). The AMP (or ADP) activation of AMPK is complicated by an interplay of phosphorylation of its α-subunit by upstream kinases (AMPKK, identified as LKB1) of the signal cascade and release of inhibition by AMP or ADP binding to the γ-subunit. As a result, the activity of AMPK can be assessed also from its phosphorylation grade. The β-subunit binds glycogen that enables the enzyme to act as a sensor of glycogen, a stored source of energy (for references, see (168).

The link between AMPK and sirtuin activity is enhanced by AMPK induction of NAMPT expression, which leads to increased synthesis and concentration of NAD^+ (39). AMPK is also able to activate phosphofructokinase, the rate-limiting enzyme of glycolysis, by phosphorylating its most powerful regulator 6-phosphofructo-2-kinase/phosphatase (104). Activation of NAD^+ synthesis upon NAMPT expression increase is advantageous also in a situation of increased NAD^+ usage during increased glycolysis (for a review on AMPK, see (16)).

In mitochondria, the sirtuin isomorphs SIRT3 and SIRT5 are significant NAD^+ consumers. SIRT3 catalyzes deacylation-based activation of acetylated, and SIRT5 of malonylated or succinylated proteins such as glutamate dehydrogenase, complex I, complex II and complex III. In the sirtuin-catalyzed reaction, NAD^+ attacks an ε-aminoacetylated lysine resulting in release of nicotinamide and 2-O-acetyl-ADP-ribose (OAADPr) which is supposed to act as a gene expression modulating agent and is further metabolized. Also mono- or polyribosylation of proteins by ADP-ribosyltransferases (ARTC) or some sirtuins consumes NAD^+. The third mitochondrial sirtuin isoform SIRT4 ADP-ribosylates glutamate dehydrogenase resulting in inhibition of the enzyme i.e. antagonizes the activating effect of SIRT3 on the same enzyme. At least 133 acetylated proteins, most of them enzymes, have been found in mouse mitochondria. It is noteworthy that ten of them are longevity-related subunits of complex I (10,48), and even the mtDNA-encoded subunit 8 of the mitochondrial ATP synthase is lysine-acetylated, which indicates that acetylation occurs also intramitochondrially. The acetylation grades of these are responsive to nutritional state (79).

The question of the role of free $[NAD^+]$/[NADH] ratio in the regulation of sirtuin action has been brought up by Lin and Guarente (95). Tree NAD^+ concentration ($[NAD^+]_f$) in a compartment is determined by the metabolism-dependent redox potential of NAD(H). The cytosolic free NAD^+/NADH ratio is about 1000 and the mitochondria near unity. Therefore the sensitivity of $[NAD^+]_f$ to redox potential change is much lower in the cytosol than in the mitochondria. Moreover, sirtuin expression the influence of NAD^+/NADH redox effects on sirtuin expression are in some cases paradoxical. Namely, mRNA and protein of SIRT1 and SIRT2 have been found to increase upon experimental increase of the cytosolic free NADH/NAD^+ ratio in hepatocytes, i.e. upon a decrease in $[NAD^+]_f$ (40). Similar is the situation in ischemia or hypoxia as sirtuin inductors, because they cause an intensive NAD^+ reduction.

There is a positive correlation between cellular concentrations of ATP and NAD^+ (30), and evidence has been presented of a signal path from NAD^+ reduction → AMPK → SIRT1 expression in hepatocytes (70). Furthermore, SIRT1 regulation of mitochondria through a PGC-1α/β-independent pathway involving the oxygen-sensitive HIF-1α system induced by a pseudohypoxia-like condition caused by NAD^+ depletion resulting in decrease of the expression of mtDNA-encoded genes (41). Conversely, NAD^+ concentration decreases during aging with concomitant decrease in the mtDNA-encoded respiratory complexes and both of these trends are alleviated in mice overexpressing the nuclear NMNAT isomorph NMNAT1. These data lend support to the view that the aging related decrease in the mitochondrial electron transfer chain activity is related to NAD^+ limitation of SIRT1 activity (41).

All this suggests that AMPK is probably a principal energy state probe for sirtuin expression and activity. NAD^+ rather serves as a co-substrate and may play a submissive role as such, although regulation of sirtuin activity by AMPK is relayed also through NAMPT effect on NAD^+ salvage synthesis as described above. The case of the primary role of NAD^+ in sirtuin activity appears to not yet been settled.

Other ADP-ribosyl transferases

The PARP group of NAD^+-consuming nuclear enzymes currently includes 17 enzymes, which play an important role in the DNA repair machinery. PARP1 is the dominant enzyme of the PARP family and preferentially binds to single strand breaks of DNA by its DNA-binding domain and initiates ADP-ribose polymerization of itself and its target proteins. PARP1 activation is one of the first responses to DNA damage and is a signal for repair synthesis. The life time of poly-ADP-ribose is short, because it is rapidly hydrolyzed to ADP-ribose and probably recycled to NAD^+ (for references, see (92,125).

Tankyrase is a PARP, which contains an Ankyrin repeat domain for protein interaction and an active site, which catalyzes poly-ADP-ribosylation (PARsylation) of several targets such as TRF1, a telomere-associated protein, which links PARsylation to chromosome end maintenance, and Axin, which normally inhibits Wnt/β-catenin signaling and promotes glucose uptake through the glucose transporter GLUT4 and the insulin-responding aminopeptidase (IRAP). The latter links Tankyrase to the GLUT4-containing vesicles by activating their insulin-stimulated exocytosis (166). It has been shown that the PARP activity of Tankyrase activity is NAD^+-limited and responds to manipulation of the nutritional condition of cells (173). AutoPARsylation of Tankyrin has also been considered a major NAD^+ sink. Because of the connection to Wnt signaling with a link to tumorigenesis Tankyrase inhibitors are currently developed for potential antineoplastic drug use (46).

CD38, is an ectoenzyme on plasma membrane of leucocytes but exists also intracellularly in subcellular vesicles. This NAD^+-consuming enzyme catalyzes the formation of the potent calcium-mobilizing molecule cyclic ADP ribose (cADPR) and its hydrolysis to ADP-ribose. To reach the CD38 ectodomain, NAD^+ escapes the cell through Connexin 43 channels. CD38/NAD^+/cADPR signaling participates in regulation of intracellular calcium and trafficking of leucocytes in response to chemoattractants and paracrine signaling (for references, see (27,99)).

ADP-ribosyl transferases, aging and longevity

ADP-ribosyl transferases represent a double-edged sword because they consume NAD^+. Dietary NAD^+ precursor supplementation that increases the NAD^+ concentration, causes SIRT1 activation and longevity in mice (170) and the nematode *Caenorhabditis elegans* (108). On one hand, aging is linked to a decrease in cellular NAD^+ and sirtuin inactivation, and on the other, inactivation of the poly-ADP-ribosyl-polymerase PARP1 increases NAD^+ availability and activates SIRT1. A relation between PARP activity and longevity has been proposed (108). However, data about the role of SIRT1 in increasing lifespan are at variance. Overexpression of SIRT1 has been found not to increase lifespan in mice (57), although evidence exists that SIRT6 is related to base excision repair of DNA and that deletion of SIRT6 results in a progeria-like syndrome in mice (107). However, brain-specific overexpression of SIRT1 in mice enhances the life-extending effect of diet restriction (DR) by upregulating type 2 orexin receptors, which also are known to augment the response to ghrelin, a gut hormone causing a hunger sensation (129). Moreover, oral administration of a ghrelin agonist has been found to inhibit cognitive decline in a murine amyloid precursor protein mutation

model of Alzheimer disease, suggesting that plain hunger is sufficient to produce similar metabolic response as DR (31).

NAD(P)-linked signaling and disease, inflammation and cell death

Nicotinamide adenine nucleotides are linked to pathologies in multiple ways. Nutritional niacin deficiency causes a variety of damages (38), and mutations in enzymes of the *de novo* $NAD(P)^+$ synthesis pathway have been documented to give rise to malformations (136). NAD^+ availability may also be involved in the pathogenesis of glaucoma, as indicated by the declining NAD^+ and NADH concentrations in retinal ganglia during progression of glaucoma (160). The slow Wallerian degeneration gene (Wld^S), is a product of a mutation that brings about a chimera with an N-terminal fraction from the ubiquitination factor Ube4b and a C-terminal fraction from the NMN adenylyltransferase (NMNAT1), and in Wld^S mice nicotinamide supplementation is neuroprotective in the retina (160).

The expression of the mitochondrial SIRT3 isomorph is regulated by the transcriptional co-activator PGC-1α which in turn has been found downregulated in mouse models of the amyotrophic lateral sclerosis (ALS) and Huntington (HD) disease. In postmortem CNS samples from ALS and HD patients the PGC-1α and SIRT3 levels shift to opposite directions: In human ALS spinal cords the SIRT3 content increases, but in HD cerebellum and striatum the levels are not different from controls. In summary, the PGC-1α and SIRT3 changes are small, and the published data do not lend solid support to a hypothesis of SIRT3 involvement in the pathogenesis of ALS or HD (13).

The pathogenesis of AD includes accumulation of β-amyloid plagues and neurofibrillary tangles generated by proteolytic cleavage of the membrane protein amyloid precursor protein (APP). Neurofibrillary tangles increase during aging and (β-A) accelerates their accumulation. Possibilities for treatment are limited and consist of acetylcholine esterase inhibitors, N-methyl-D-aspartate receptor antagonists and immunological procedures to enhance dissolving of the tangles, although success is negligible.

Transgenic animal models of AD have shown that caloric restriction is protective against ailments related to aging, AD and ALS. In AD- or ALS-susceptible transgenic mice, SIRT1 expression increases during progress of the disease, indicating that SIRT1 is a stressor-induced enzyme. Sirtuin expression can be activated by drugs of the polyphenol category including resveratrol, and injection of resveratrol into cerebral ventricles of AD-susceptible mice increases SIRT1 expression and slows neurodegeneration and decline of associative learning (78). In a human study for estimating resveratrol safety, where β-A metabolite concentrations and brain pseudoatrophy were assessed, it was found that high dosage of the drug was necessary to obtain significant CNS concentrations, and the biomarker changes still were small (148).

SIRT 1 responds to inflammation (for references, see (149)) and is involved in initiation of protective actions such as autophagy to eliminate damaged cell organelles, where the PI3K/Akt/mTOR signal path and direct deacetylation of the autophagy gene products (87) are involved. Even starvation-induced SIRT1 activation results in deacetylation of autophagy-related genes to adjust autophagy to the metabolic situation (87). However, continual, adaptive, elevated SIRT1 activity during inflammation may lead to prolongation of the condition (149).

Sirtuins are protective against cancer and their mutations tumorigenic (56), but pharmacologic SIRT inhibition has been shown to restrain tumor growth by destabilizing tumor DNA. Potent inhibitors of particular sirtuins have been found and are under investigation (72).

Continuous monitoring of redox potential of nicotinamide adenine nucleotides

Compartmentation and detectability

Optical monitoring of redox organization of living tissues has gained increasing awareness, because NADH and NADPH are fluorescent when excited at a near-UV band. They both have an absorbance maximum at 340 nm and emission maximum at 460 nm. For investigation of intact cells and organs a new dimension of fluorescence monitoring of NAD(P)H is afforded by two-photon excitation with near-IR wavelengths around 700 nm, which avoids UV damage of the target, penetrates deeper (1 mm) in the tissue and has an advantage in 3D imaging of the reduction grade of nicotinamide nucleotides (68,154,167).

Although the optical spectra of NADH and NADPH are similar, they can be differentiated by fluorescence lifetime with the two-photon excitation technology. However, this applies only for the enzyme-bound nucleotides (9). Moreover, the multiphoton fluorescence lifetime imaging has recently revealed that SIRT2 controls sub-organellar compartmentation of bound NADH in the nucleus (3). It has been suggested that the shortening of fluorescence lifetime of bound and free NADH is caused by an increase of the NADH/NAD^+ ratio (7).

Compartment-specific spectroscopic monitoring of free NADH is problematic in mitochondrion-rich organs such as heart muscle. The cytosolic free NADH concentration is too low for significant contribution to the changes in total nicotinamide nucleotide absorbance (11). Under most conditions, fluorescence of a nicotinamide coenzyme to an enzyme results in fluorescence enhancement, but is depends on the attainment of the conformation (open or closed) of the nicotinamide ring upon binding (34). Examples of contrasting behavior exist (66,153). Success in monitoring of cytosolic NAD(P)H depends on the density of the mitochondrial population. In experiments where perfused heart surface NAD(P)H fluorescence was titrated with varying extracellular [lactate]/[pyruvate] (L/P) ratio the fluorescence changes are proportional to the pyruvate concentration but not to L/P ratio, indicating that the redox effect of pyruvate oxidation swamps the cytosolic NAD(P)H fluorescence changes (113) that is in agreement with data from isolated cardiac papillary muscle (21). However, in a similar L/P ratio titration of isolated perfused rat liver (113) the surface NAD(P)H fluorescence increase was proportional to the extracellular L/P ratio, showing that LDH near-equilibrium is the main determinant of the hepatic NADH fluorescence signal in agreement with the data of Bücher and coworkers (11,139).

The FAD prosthetic group of the lipoamide dehydrogenases is in near-equilibrium with the free NADH/NAD^+ pool in mitochondria (52) so that the $FADH_2$/FAD ratio qualitatively reflects the NADH/NAD^+ ratio. (52,86). FAD in the dihydrolipoamide dehydrogenase and NAD^+ represent almost similar mid-potentials (52,101,163) so that, their redox ratios are almost identical under near-equilibrium conditions. FAD is fluorescent at 470 nm excitation and emits at about 520 nm, but its reduced form $FADH_2$ is non-fluorescent. Therefore, the fluorescences of FAD and NAD change in opposite directions upon reduction. Because lipoamide dehydrogenase is the dominant fluorescent flavoprotein in cells, it can be used as a compartment-specific mitochondrial indicator of the free NADH/NAD^+ ratio (51,52). Moreover, the NADH/FAD fluorescence ratio presents a means of increasing the sensitivity and decreasing the artefact caused by changes in attenuation of fluorescence in intact tissues (132).

Some derivatives of the dual monitoring are used, e.g. the “normalized” NADH/(flavin+NADH) or flavin/(flavin+NADH) fluorescence ratios, which are less affected by hemodynamic changes in tissues (91,165). Possibilities of compartment-specific fluorescence monitoring of NADH are organ specific, as described above (21,113).

The normalized fluorescence ratio method of artifact elimination has been tested in a two-photon fluorescence excitation imaging setup in engineered normal or precancerous 3D epithelial tissue

models combined with liquid chromatography/tandem mass spectrometric analysis of cellular NAD(H) and FAD(H_2) and correction of the fluorescence data for background fluorescence of keratin (152). The chemical determination data of the endogenous fluorophores well correlated with the normalized fluorescence ratio, particularly after elimination of the basal keratin fluorescence by statistical methods. Moreover, the redox ratio pattern varied between different precancerous models (152). Further studies may show the potential of redox imaging in cancer diagnostics.

Although the combined ^{31}P NMR signal of NADH and NAD^+ has been identified *in vivo* and *ex vivo* with spectrometry of intact organs, the overlapping signals are too close to the base of the α-phosphate peak of ATP and therefore considered too weak for quantitative analysis. However, it has been recently demonstrated that by using high-field spectrometers and sophisticated deconvolution and modeling it is possible to quantitate NADH and NAD^+ and NAD^+/NADH ratio in cat or human brain in vivo (97,174).

Although ^{31}P NMR resonances of $NADP^+$ and NADPH are riding at the foot of the α-ATP peak, their resonances and their compartmental ratio can be distinguished in vivo in human tight muscle by careful extraction of the nicotinamide nucleotide phosphate peak region and measuring their magnitude changes upon changes in mitochondrial population density and fitness of the test subject upon exercise training (24).

Recently also ^{1}H NMR has been successfully applied to NAD^+ measurement in rat cerebral cortex (28). However, it is unavoidable to select an excitation pulse center which also suppresses water signal, and due to cross-relaxation between water and NAD^+ this water suppression diminishes also the NAD^+ signal. Therefore a special technique is needed for elimination of the water interference and converting the NAD^+ signal to absolute concentrations. NADH could not be detected by ^{1}H-NMR, because its signal overlaps the signal of glutamine and other amines (28).

Transgenic fluorescent probes for monitoring of NADH/NAD⁺ ratio

Recently several genetically encoded NADH/NAD redox ratio probes have been developed (reviewed in (98)). With related methodologies, it has been demonstrated that mitochondrial $[Ca^{2+}]_f$-induced matrix NADH increase is transmitted to the cytosolic NADH/NAD^+ ratio, which in turn increases cytosolic SIRT1 expression and consequent protein deacetylation. Although it is generally considered that the nutrition-related sirtuin activity changes are dependent on NAD^+ concentration determined by the NADH/NAD^+ ratio, a compensatory increase in cytosolic SIRT1 expression can be induced by an increase in the NADH/NAD^+ ratio with concomitant decrease in NAD^+ (102).

Indicator enzyme and redox metabolite approach

Compartment-specific measurement of redox ratio of the free forms of the nicotinamide-adenine nucleotides can be performed, when a strictly compartmentalized NAD^+-linked enzyme with sufficient activity to attain a near-equilibrium condition is available. A canonical example is the liver mitochondrial 3-hydroxybutyrate dehydrogenase (BDH1), which catalyzes the reaction

$$3\text{-}hydroxybutyrate + NAD^+ \leftrightarrow acetoacetate + NADH + H^+$$

Production of 3-hydroxybutyrate (βOHB) from acetoacetate (AcAc) during ketogenesis in liver is a metabolic dead-end, because acetoacetate is not readily oxidized in that organ, so that BDH1 attains a near-equilibrium. Under ketogenic conditions the excess of acetyl-CoA in liver is condensed to acetoacetyl-CoA, which is further converted to free acetoacetate and reduced to 3-hydroxybutyrate to match the mitochondrial NADH/NAD^+ ratio. The mixture is exported to blood and used in extrahepatic tissues. Thus the βOHB/AcAc ratio in blood reflects the NADH/NAD^+ ratio of hepatic mitochondria. However, a cytosolic 3-hydroxybutyrate dehydrogenase encoded by

the BDH2 gene has been recently described (45,103). The BDH2 activity is an L-3-hydroxybutyrate dehydrogenase, i.e. its isomer specificity is opposite to that of BDH1 (58).

The βOHB /AcAc ratio cannot be used as a mitochondrial NADH/NAD^+ ratio indicator in heart muscle, which has high AcAc oxidation activity. Although opinions about the near-equilibrium balance of glutamate dehydrogenase in cardiac muscle have been at variance (116), reactants of glutamate dehydrogenase in the isolated perfused rat heart have been validated as indicators of the redox ratio of mitochondrial NADH/NAD^+ (114) and employed to calibrate optical readout of mitochondrial NADH/NAD^+ (53).

Conclusions

In addition to their primary role in hydride transfer in redox reactions and as a substrate for conversion of the combustion energy by ETC, the nicotinamide-adenine nucleotides participates in regulation of energy metabolism. In these assignments they serve as co-substrates, allosteric activators and feedback inhibitors, substrate activators, product inhibitors, sensors of nutritional state, regulators of post-translational modification, modulators of gene expression and DNA repair.

Normal redox ratios of [NAD(P)H]/[$NAD(P)^+$] are linked to supply of reducing equivalents for reductive syntheses and also to physiological production of reactive oxygen or nitrogen species. Out-of-range ratios may lead to oxidative stress.

The nicotinamide nucleotides are not only redox mediators, but are exploited in reactions which use their degradation as a source of energy. This necessitates subsequent salvage synthesis of the nucleotides.

Revelation of the substrate role of nicotinamide adenine nucleotides in deacetylation and deacylation of proteins by sirtuins, has provided new insight to the signal paths leading to cell protection, elimination of damaged cell organelles by autophagy and delaying senescence.

.Abbreviations Used

Akt	=	protein kinase B	NADK2	=	mitochondrial NAD kinase
AMPK	=	AMP-dependent protein kinase	Nam	=	nicotinamide
ART	=	ADP ribosyltransferase			
BDH1	=	3-hydroxybutyrate dehydrogenase, type 1	NAMPT	=	nicotinamide/nicotinic acid mononucleotide adenylyltransferase
BDH2	=	3-hydroxybutyrate dehydrogenase, type 2	NamR	=	nicotinamide riboside
DECR	=	2,4-dienoyl-CoA reductase	NMN	=	nicotinamide mononucleotide
DOAP	=	dihydroxyacetone phosphate	NMNAT	=	nicotinamide mononucleotide adenylyl transferase
E1	=	pyruvate dehydrogenase	NRK1, 2	=	nicotinamide riboside kinases 1, 2
E2	=	dihydrolipoamide acetyltransferase	NUDT12	=	hydrolase of the Nudix family of pyrophosphatases
E3	=	dihydrolipoamide dehydrogenase	OGDH	=	2-oxoglutarate dehydrogenase
ERO1	=	endoplasmic reticulum luminal thiol oxidase	OxAc	=	oxaloacetate
G3P	=	glycerol-3-phosphate	PARP	=	poly-ADP-ribosyl-polymerase
G3PDH	=	glycerol-3-phosphate dehydrogenase	PDC	=	pyruvate dehydrogenase complex
G6PDH	=	glucose-6-phosphate dehydrogenase	PDH	=	pyruvate dehydrogenase
GSH	=	reduced glutathione	PDI	=	protein disulfide isomerase
GSSG	=	oxidized glutathione	PDK1-4	=	pyruvate dehydrogenase kinases 1 to 4
IDH1	=	cytosolic NADP-linked isocitrate dehydrogenase	PDP1-2	=	pyruvate dehydrogenase phosphate phosphatases 1 and 2
IDH2	=	mitochondrial NADP-linked isocitrate dehydrogenase	PGC-1α	=	peroxisome proliferator-activated receptor gamma coactivator 1-α
IDH3	=	mitochondrial NAD-linked isocitrate dehydrogenase	P_i	=	inorganic phosphate
LDHB	=	lactate dehydrogenase subunit B	PI3K	=	phosphoinositide 3-kinase
LDHBx	=	read-through-extended lactate dehydrogenase subunit B	PPP	=	pentose phosphate pathway
MAL	=	malate	PRDX4	=	peroxiredoxin 4
MDH	=	malate dehydrogenase	PXMP2	=	peroxisomal membrane protein 2 (channel)
MDHx	=	read-through-extended malate dehydrogenase	PXN	=	plant peroxisomal NAD^+ translocator
ME1	=	cytosolic malic enzyme	QA	=	quinolinic acid
ME2	=	mitochondrial malic enzyme	QPRT	=	quinolinate phosphoribosyltransferase
mtGPDH	=	mitochondrial glycerol-3-phosphate:ubiquinone oxidoreductase	SIRT1-7	=	sirtuins 1 to 7
mTOR	=	mammalian target of rapamycin	TCA	=	tricarboxylic acid
mTOR	=	mammalian target of rapamycin			
$\Delta\tilde{\mu}H^+$	=	electrochemical potential of protons			

Legends to figures

FIG. 1. Main NAD$^+$- and NADP$^+$-linked pathways of energy metabolism. Key enzymes of TCA cycle, gluconeogenesis, glycolysis, fatty acid oxidation and substrate provision for lipogenesis. CL, citrate lyase; PDH, pyruvate dehydrogenase complex; PC, pyruvate carboxylase; CS, citrate synthase; IDH1, cytosolic NADP$^+$-linked isocitrate dehydrogenase; IDH2, mitochondrial NADP$^+$-linked isocitrate dehydrogenase; IDH3, GOT2, mitochondrial aspartate transaminase; OGDH, 2-oxoglutarate dehydrogenase; STK, succinate thiokinase; SDH, succinate dehydrogenase; FH, fumarate hydratase; MDH1, cytosolic NAD$^+$-linked malate dehydrogenase; MDH2 mitochondrial NAD$^+$-linked malate dehydrogenase; ME1, cytosolic malic enzyme; ME3, mitochondrial malic enzyme.

FIG. 2. Transfer of reducing equivalents from cytosolic NADH to the mitochondrial matrix against a redox gradient by the electrogenic malate-aspartate shuttle. The numerical values describing the redox poise in cytosol and mitochondrial matrix represent a metabolic situation in an isolated perfused rat heart (114).

FIG .3. Redox potential- and energy-linked control of main catabolic pathways. The dashed arrows depict regulatory interactions. Mass-action equation of the adenylate kinase reaction is displayed to emphasize the amplification built in its $[ADP]^2$ term. AMPK, AMP-dependent protein kinase; GDH, glutamate dehydrogenase; OGDH, 2-oxoglutarate dehydrogenase; MDH3, NAD$^+$-linked malate dehydrogenase; IDH3, NAD$^+$-linked isocitrate dehydrogenase; CS, citrate synthase; PDH, pyruvate dehydrogenase complex; OxAc, oxaloacetate.

FIG. 4. NAD$^+$ and NADP$^+$ biosynthesis in cytosol, and consumption and salvage in mitochondria. Trp, tryptophan; QA, quinolinic acid; QPRT, quinolinate phophoribosyltransferase; Na, nicotinic acid; NaPT, nicotinic acid phosphoribosyltransferase; NMNAT, nicotinamide/nicotinic acid mononucleotide adenylyltransferase; NADS, NAD synthase; NaMN, nicotinic acid mononucleotide; Nam, nicotinamide; NamPT, nicotinamide phosphoribosyltransferase; NR, nicotinamide riboside; NRK, nicotinamide riboside kinase; NMAT1-2, nuclear and cytosolic nicotinamide mononucleotide adenylyltransferase isoforms 1 and 2; NMAT3, mitochondrial nicotinamide mononucleotide adenylyltransferase isoform 3; GDH, glutamate dehydrogenase; NADK1, cytosolic NAD$^+$ kinase isoform; NADK2, mitochondrial NAD$^+$ kinase isoform.

FIG. 5. Mitochondria and peroxisomes collaborate in metabolism and biogenesis. (1) In the absence of peroxisomes the peroxins (peroxisomal assembly proteins) synthetized in the endoplasmic reticulum (2) are mistargeted to mitochondria. (3) *De novo* peroxisomes formed in the endoplasmic reticulum (4) make contact with the mitochondrial membrane to acquire a peroxin (Pex1) and parts of mitochondrial membrane (mitochondrion-derived vesicles) (5) to obtain competence for peroxisome maturation. Oxidation of very long-chain fatty acids (VLCFA, 22-28 carbon atoms) necessitates participation of peroxisomes because mitochondria are devoid of VLCFA CoA synthetase. Peroxisomal fatty acid oxidase system shortens the fatty acid molecule to a length acceptable by the mitochondrial acyl-CoA synthetase. CROT, carnitine octanoate transferase. For the redox substrate shuttle components, see Fig. 6.

FIG. 6. Peroxisomal transmembrane traffic of reducing equivalents and pool size maintenance of NADH/NAD$^+$. The membrane pores are permeable to small molecules so that some substrate shuttles operate without specific metabolite translocators. LDHx and MDH1x stand for translation read-through-extended forms of lactate and malate dehydrogenases, respectively. G3P, DOAP and GPDH stand for glycerol-3-phosphate, dihydroxyacetone phosphate and glycerol-3-phosphate dehydrogenase, respectively.

1. Abdelraheim SR, Spiller DG and McLennan AG. Mammalian NADH diphosphatases of the Nudix family: cloning and characterization of the human peroxisomal NUDT12 protein. *Biochem J* 374: 329-335, 2003.

2. Agrimi G, Russo A, Scarcia P and Palmieri F. The human gene SLC25A17 encodes a peroxisomal transporter of coenzyme A, FAD and NAD^+. *Biochem J* 443: 241-247, 2012.

3. Aguilar-Arnal L, Ranjit S, Stringari C, Orozco-Solis R, Gratton E and Sassone-Corsi P. Spatial dynamics of SIRT1 and the subnuclear distribution of NADH species. *Proc Natl Acad Sci U S A* 113: 12715-12720, 2016.

4. Antonenkov VD and Hiltunen JK. Transfer of metabolites across the peroxisomal membrane. *Biochim Biophys Acta* 1822: 1374-1386, 2012.

5. Antonenkov VD, Sormunen RT and Hiltunen JK. The rat liver peroxisomal membrane forms a permeability barrier for cofactors but not for small metabolites in vitro. *J Cell Sci* 117: 5633-5642, 2004.

6. Atkinson DE. The energy charge of the adenylate pool as a regulatory parameter. Interaction with feedback modifiers. *Biochemistry* 7: 4030-4034, 1968.

7. Bird DK, Yan L, Vrotsos KM, Eliceiri KW, Vaughan EM, Keely PJ, White JG and Ramanujam N. Metabolic mapping of MCF10A human breast cells via multiphoton fluorescence lifetime imaging of the coenzyme NADH. *Cancer Reseach* 65: 8766-8773, 2005.

8. Bizouarn T, Meuller J, Axelsson M and Rydström J. The transmembrane domain and the proton channel in proton-pumping transhydrogenases. *Biochim Biophys Acta* 1459: 284-290, 2000.

9. Blacker TS and Duchen MR. Investigating mitochondrial redox state using NADH and NADPH autofluorescence. *Free Radic Biol Med* 100: 53-65, 2016.

10. Browner WS, Kahn AJ, Ziv E, Reiner AP, Oshima J, Cawthon RM, Hsueh WC and Cummings SR. The genetics of human longevity. *Am J Med* 117: 851-860, 2004.

11. Bücher T, Brauser B, Conze A, Klein F, Langguth O and Sies H. State of oxidation-reduction and state of binding in the cytosolic NADH-system as disclosed by equilibration with extracellular lactate-pyruvate in hemoglobin-free perfused rat liver. *Eur J Biochem* 27: 301-317, 1972.

12. Bücher T and Klingenberg M. Wege des Wasserstoffs in der lebendigen Organisation. *Angew Chem* 70: 552-570, 1958.

13. Buck E, Bayer H, Lindenberg KS, Hanselmann J, Pasquarelli N, Ludolph AC, Weydt P and Witting A. Comparison of Sirtuin 3 Levels in ALS and Huntington's Disease-Differential Effects in Human Tissue Samples vs. Transgenic Mouse Models. *Front Mol Neurosci* 10: 156, 2017.

14. Canto C, Gerhart-Hines Z, Feige JN, Lagouge M, Noriega L, Milne JC, Elliott PJ, Puigserver P and Auwerx J. AMPK regulates energy expenditure by modulating NAD$^+$ metabolism and SIRT1 activity. *Nature* 458: 1056-1060, 2009.

15. Canto C, Menzies KJ and Auwerx J. NAD$^+$ metabolism and the control of energy homeostasis: A balancing act between mitochondria and the nucleus. *Cell Metab* 22: 31-53, 2015.

16. Carling D, Thornton C, Woods A and Sanders MJ. AMP-activated protein kinase: new regulation, new roles? *Biochem J* 445: 11-27, 2012.

17. Casazza JP and Veech RL. The content of pentose-cycle intermediates in liver in starved, fed ad libitum and meal-fed rats. *Biochem J* 236: 635-641, 1986.

18. Chance B. The composition of catalase-peroxide complexes. *J Biol Chem* 179: 1311-1330, 1949.

19. Chance B. An intermediate compound in the catalase-hydrogen peroxide reaction. *Acta Chem Scand* 1: 236-267, 1947.

20. Chance B, Sies H and Boveris A. Hydroperoxide metabolism in mammalian organs. *Physiol Rev* 59: 527-605, 1979.

21. Chapman JB. Fluorometric studies of oxidative metabolism in isolated papillary muscle of the rabbit. *J Gen Physiol* 59: 135-154, 1972.

22. Ciccarese F and Ciminale V. Escaping death: Mitochondrial redox homeostasis in cancer cells. *Front Oncol* 7: 117, 2017.

23. Colussi T, Parsonage D, Boles W, Matsuoka T, Mallett TC, Karplus PA and Claiborne A. Structure of alpha-glycerophosphate oxidase from *Streptococcus sp*.: a template for the mitochondrial alpha-glycerophosphate dehydrogenase. *Biochemistry* 47: 965-977, 2008.

24. Conley KE, Ali AS, Flores B, Jubrias SA and Shankland EG. Mitochondrial NAD(P)H in vivo: Identifying natural indicators of oxidative phosphorylation in the ^{31}P magnetic resonance spectrum. *Front Physiol* 7: 45, 2016.

25. Couto N, Wood J and Barber J. The role of glutathione reductase and related enzymes on cellular redox homoeostasis network. *Free Radic Biol Med* 95: 27-42, 2016.

26. Crabtree B and Newsholme EA. The activities of phosphorylase, hexokinase, phosphofructokinase, lactate dehydrogenase and the glycerol 3-phosphate dehydrogenases in muscles from vertebrates and invertebrates. *Biochem J* 126: 49-58, 1972.

27. De Flora A, Zocchi E, Guida L, Franco L and Bruzzone S. Autocrine and paracrine calcium signaling by the CD38/NAD$^+$/cyclic ADP-ribose system. *Ann N Y Acad Sci* 1028: 176-191, 2004.

28. de Graaf RA and Behar KL. Detection of cerebral NAD^+ by in vivo ^1H NMR spectroscopy. *NMR Biomed* 27: 802-809, 2014.

29. Denton RM, Pullen TJ, Armstrong CT, Heesom KJ and Rutter GA. Calcium-insensitive splice variants of mammalian E1 subunit of 2-oxoglutarate dehydrogenase complex with tissue-specific patterns of expression. *Biochem J* 473: 1165-1178, 2016.

30. Devin A, Guerin B and Rigoulet M. Cytosolic NAD^+ content strictly depends on ATP concentration in isolated liver cells. *FEBS Lett* 410: 329-332, 1997.

31. Dhurandhar EJ, Allison DB, van Groen T and Kadish I. Hunger in the absence of caloric restriction improves cognition and attenuates Alzheimer's disease pathology in a mouse model. *PLoS One* 8: e60437, 2013.

32. Di Lisa F and Ziegler M. Pathophysiological relevance of mitochondria in NAD^+ metabolism. *FEBS Lett* 492: 4-8, 2001.

33. Di Noia MA, Todisco S, Cirigliano A, Rinaldi T, Agrimi G, Iacobazzi V and Palmieri F. The human SLC25A33 and SLC25A36 genes of solute carrier family 25 encode two mitochondrial pyrimidine nucleotide transporters. *J Biol Chem* 289: 33137-33148, 2014.

34. Dugan RE and Porter JW. Mechanism of binding of reduced nicotinamide adenine dinucleotide phosphate to vertebrate fatty acid synthetases. *J Biol Chem* 246: 637-642, 1971.

35. Eggleston LV and Krebs HA. Regulation of the pentose phosphate cycle. *Biochem J* 138: 425-435, 1974.

36. Forsander OA. Influence of some aliphatic alcohols on the metabolism of rat liver slices. *Biochem J* 105: 93-97, 1967.

37. Fransen M, Lismont C and Walton P. The peroxisome-mitochondria connection: How and why? *Int J Mol Sci* 18: 10.3390/ijms18061126, 2017.

38. Fu L, Doreswamy V and Prakash R. The biochemical pathways of central nervous system neural degeneration in niacin deficiency. *Neural Regen Res* 9: 1509-1513, 2014.

39. Fulco M, Cen Y, Zhao P, Hoffman EP, McBurney MW, Sauve AA and Sartorelli V. Glucose restriction inhibits skeletal myoblast differentiation by activating SIRT1 through AMPK-mediated regulation of Nampt. *Dev Cell* 14: 661-673, 2008.

40. Gambini J, Gomez-Cabrera MC, Borras C, Valles SL, Lopez-Grueso R, Martinez-Bello VE, Herranz D, Pallardo FV, Tresguerres JA, Serrano M and Vina J. Free [NADH]/[NAD^+] regulates sirtuin expression. *Arch Biochem Biophys* 512: 24-29, 2011.

41. Gomes AP, Price NL, Ling AJ, Moslehi JJ, Montgomery MK, Rajman L, White JP, Teodoro JS, Wrann CD, Hubbard BP, Mercken EM, Palmeira CM, de Cabo R, Rolo AP, Turner N, Bell EL and Sinclair DA. Declining NAD^+ induces a pseudohypoxic state disrupting nuclear-mitochondrial communication during aging. *Cell* 155: 1624-1638, 2013.

42. Gonfloni S, Iannizzotto V, Maiani E, Bellusci G, Ciccone S and Diederich M. P53 and Sirt1: routes of metabolism and genome stability. *Biochem Pharmacol* 92: 149-156, 2014.

43. Gout E, Rebeille F, Douce R and Bligny R. Interplay of Mg^{2+}, ADP, and ATP in the cytosol and mitochondria: unravelling the role of Mg^{2+} in cell respiration. *Proc Natl Acad Sci U S A* 111: E4560-7, 2014.

44. Guo J, Hezaveh S, Tatur J, Zeng AP and Jandt U. Reengineering of the human pyruvate dehydrogenase complex: from disintegration to highly active agglomerates. *Biochem J* 474: 865-875, 2017.

45. Guo K, Lukacik P, Papagrigoriou E, Meier M, Lee WH, Adamski J and Oppermann U. Characterization of human DHRS6, an orphan short chain dehydrogenase/reductase enzyme: a novel, cytosolic type 2 R-beta-hydroxybutyrate dehydrogenase. *J Biol Chem* 281: 10291-10297, 2006.

46. Haikarainen T, Waaler J, Ignatev A, Nkizinkiko Y, Venkannagari H, Obaji E, Krauss S and Lehtiö L. Development and structural analysis of adenosine site binding tankyrase inhibitors. *Bioorg Med Chem Lett* 26: 328-333, 2016.

47. Hallows WC, Lee S and Denu JM. Sirtuins deacetylate and activate mammalian acetyl-CoA synthetases. *Proc Natl Acad Sci U S A* 103: 10230-10235, 2006.

48. Hamilton B, Dong Y, Shindo M, Liu W, Odell I, Ruvkun G and Lee SS. A systematic RNAi screen for longevity genes in *C. elegans*. *Genes Dev* 19: 1544-1555, 2005.

49. Hasan NM, Longacre MJ, Stoker SW, Kendrick MA and MacDonald MJ. Mitochondrial malic enzyme 3 is important for insulin secretion in pancreatic beta-cells. *Mol Endocrinol* 29: 396-410, 2015.

50. Hassinen I and Kähönen MT. Hydrogen peroxide formation and catalase regulation in rats treated with ethyl-alpha-p-chlorophenoxy-isobutyrate (clofibrate). In: *Alcohol and aldehyde metabolizing systems*, edited by Thurman RG, Yonetani T, Williamson JR and Chance B. New York: Academic Press, 1974, pp. 199-206.

51. Hassinen I. From identification of fluorescent flavoproteins to mitochondrial redox indicators in intact tissues. *J Innov Opt Health Sci* 7: 1350058-1-1350058-6, 2014.

52. Hassinen I and Chance B. Oxidation-reduction properties of the mitochondrial flavoprotein chain. *Biochem Biophys Res Commun* 31: 895-900, 1968.

53. Hassinen I, Ito K, Nioka S and Chance B. Mechanism of fatty acid effect on myocardial oxygen consumption. A phosphorus NMR study. *Biochim Biophys Acta* 1019: 73-80, 1990.

54. Hassinen IE and Hiltunen K. Respiratory control in isolated perfused rat heart. Role of the equilibrium relations between the mitochondrial electron carriers and the adenylate system. *Biochim Biophys Acta* 408: 319-330, 1975.

55. Hatahet F and Ruddock LW. Protein disulfide isomerase: a critical evaluation of its function in disulfide bond formation. *Antioxid Redox Signal* 11: 2807-2850, 2009.

56. Head PE, Zhang H, Bastien AJ, Koyen AE, Withers AE, Daddacha WB, Cheng X and Yu DS. Sirtuin 2 mutations in human cancers impair its function in genome maintenance. *J Biol Chem* 292: 9919-9931, 2017.

57. Herranz D, Munoz-Martin M, Canamero M, Mulero F, Martinez-Pastor B, Fernandez-Capetillo O and Serrano M. Sirt1 improves healthy ageing and protects from metabolic syndrome-associated cancer. *Nat Commun* 1: 3, 2010.

58. Herzberg GR and Gad M. Evidence that the cytosolic activity of 3-hydroxybutyrate dehydrogenase in chicken liver is L-3-hydroxyacid dehydrogenase. *Biochim Biophys Acta* 802: 67-70, 1984.

59. Hiltunen JK and Hassinen IE. Energy-linked regulation of the citric acid cycle and the pool size of the cycle intermediates in the isolated perfused rat heart. *Int J Biochem* 8: 505-509, 1977.

60. Hiltunen JK, Kärki T, Hassinen IE and Osmundsen H. beta-Oxidation of polyunsaturated fatty acids by rat liver peroxisomes. A role for 2,4-dienoyl-coenzyme A reductase in peroxisomal beta-oxidation. *J Biol Chem* 261: 16484-16493, 1986.

61. Hofhuis J, Schueren F, Notzel C, Lingner T, Gartner J, Jahn O and Thoms S. The functional readthrough extension of malate dehydrogenase reveals a modification of the genetic code. *Open Biol* 6: 160246, 2016.

62. Holness MJ and Sugden MC. Regulation of pyruvate dehydrogenase complex activity by reversible phosphorylation. *Biochem Soc Trans* 31: 1143-1151, 2003.

63. Honsho M, Asaoku S, Fukumoto K and Fujiki Y. Topogenesis and homeostasis of fatty acyl-CoA reductase 1. *J Biol Chem* 288: 34588-34598, 2013.

64. Hottiger MO, Hassa PO, Luscher B, Schuler H and Koch-Nolte F. Toward a unified nomenclature for mammalian ADP-ribosyltransferases. *Trends Biochem Sci* 35: 208-219, 2010.

65. Houten SM, Denis S, Te Brinke H, Jongejan A, van Kampen AH, Bradley EJ, Baas F, Hennekam RC, Millington DS, Young SP, Frazier DM, Gucsavas-Calikoglu M and Wanders RJ. Mitochondrial NADP(H) deficiency due to a mutation in NADK2 causes dienoyl-CoA reductase deficiency with hyperlysinemia. *Hum Mol Genet* 23: 5009-5016, 2014.

66. Hsu RY and Lardy HA. Pigeon liver malic enzyme. 3. Fluorescence studies of coenzyme binding. *J Biol Chem* 242: 527-532, 1967.

67. Hua T, Wu D, Ding W, Wang J, Shaw N and Liu ZJ. Studies of human 2,4-dienoyl CoA reductase shed new light on peroxisomal beta-oxidation of unsaturated fatty acids. *J Biol Chem* 287: 28956-28965, 2012.

68. Huang S, Heikal AA and Webb WW. Two-photon fluorescence spectroscopy and microscopy of NAD(P)H and flavoprotein. *Biophys J* 82: 2811-2825, 2002.

69. Iacobazzi V, Infantino V, Castegna A, Menga A, Palmieri EM, Convertini P and Palmieri F. Mitochondrial carriers in inflammation induced by bacterial endotoxin and cytokines. *Biol Chem* 398: 303-317, 2016.

70. Ido Y. Diabetic complications within the context of aging: Nicotinamide adenine dinucleotide redox, insulin C-peptide, sirtuin 1-liver kinase B1-adenosine monophosphate-activated protein kinase positive feedback and forkhead box O3. *J Diabetes Investig* 7: 448-458, 2016.

71. Jeninga EH, Schoonjans K and Auwerx J. Reversible acetylation of PGC-1: connecting energy sensors and effectors to guarantee metabolic flexibility. *Oncogene* 29: 4617-4624, 2010.

72. Jiang Y, Liu J, Chen D, Yan L and Zheng W. Sirtuin inhibition: Strategies, inhibitors, and therapeutic potential. *Trends Pharmacol Sci* 38: 459-472, 2017.

73. Jones AJ, Blaza JN, Varghese F and Hirst J. Respiratory Complex I in *Bos taurus* and *Paracoccus denitrificans* pumps four protons across the membrane for every NADH oxidized. *J Biol Chem* 292: 4987-4995, 2017.

74. Jones DP and Sies H. The Redox Code. *Antioxid Redox Signal* 23: 734-746, 2015.

75. Kahn BB, Alquier T, Carling D and Hardie DG. AMP-activated protein kinase: ancient energy gauge provides clues to modern understanding of metabolism. *Cell Metab* 1: 15-25, 2005.

76. Kärki T, Hakkola E, Hassinen IE and Hiltunen JK. Beta-oxidation of polyunsaturated fatty acids in peroxisomes. Subcellular distribution of delta 3,delta 2-enoyl-CoA isomerase activity in rat liver. *FEBS Lett* 215: 228-232, 1987.

77. Kauppinen RA, Hiltunen JK and Hassinen IE. Mitochondrial membrane potential, transmembrane difference in the NAD^+ redox potential and the equilibrium of the glutamate-aspartate translocase in the isolated perfused rat heart. *Biochim Biophys Acta* 725: 425-433, 1983.

78. Kim D, Nguyen MD, Dobbin MM, Fischer A, Sananbenesi F, Rodgers JT, Delalle I, Baur JA, Sui G, Armour SM, Puigserver P, Sinclair DA and Tsai LH. SIRT1 deacetylase protects against neurodegeneration in models for Alzheimer's disease and amyotrophic lateral sclerosis. *EMBO J* 26: 3169-3179, 2007.

79. Kim SC, Sprung R, Chen Y, Xu Y, Ball H, Pei J, Cheng T, Kho Y, Xiao H, Xiao L, Grishin NV, White M, Yang XJ and Zhao Y. Substrate and functional diversity of lysine acetylation revealed by a proteomics survey. *Mol Cell* 23: 607-618, 2006.

80. Klingenberg M. Localization of the glycerol-phosphate dehydrogenase in the outer phase of the mitochondrial inner membrane. *Eur J Biochem* 13: 247-252, 1970.

81. Klingenberg M. Mitochondria metabolite transport. *FEBS Lett* 6: 145-154, 1970.

82. Kok BP, Venkatraman G, Capatos D and Brindley DN. Unlike two peas in a pod: lipid phosphate phosphatases and phosphatidate phosphatases. *Chem Rev* 112: 5121-5146, 2012.

83. Krebs HA, Freedland RA, Hems R and Stubbs M. Inhibition of hepatic gluconeogenesis by ethanol. *Biochem J* 112: 117-124, 1969.

84. Kruger NJ and von Schaewen A. The oxidative pentose phosphate pathway: structure and organisation. *Curr Opin Plant Biol* 6: 236-246, 2003.

85. Kuhlbrandt W. Structure and function of mitochondrial membrane protein complexes. *BMC Biol* 13: 89-015-0201-x, 2015.

86. Kunz WS. Spectral properties of fluorescent flavoproteins of isolated rat liver mitochondria. *FEBS Lett* 195: 92-96, 1986.

87. Lee IH, Cao L, Mostoslavsky R, Lombard DB, Liu J, Bruns NE, Tsokos M, Alt FW and Finkel T. A role for the NAD-dependent deacetylase Sirt1 in the regulation of autophagy. *Proc Natl Acad Sci U S A* 105: 3374-3379, 2008.

88. Lee YP and Lardy HA. Influence of thyroid hormones on L-alpha-glycerophosphate dehydrogenases and other dehydrogenases in various organs of the rat. *J Biol Chem* 240: 1427-1436, 1965.

89. Lehtonen MA, Savolainen MJ and Hassinen IE. Hormonal regulation of hepatic soluble phosphatidate phosphohydrolase. Induction by cortisol in vivo and in isolated perfused rat liver. *FEBS Lett* 99: 162-166, 1979.

90. Leyssens A, Nowicky AV, Patterson L, Crompton M and Duchen MR. The relationship between mitochondrial state, ATP hydrolysis, $[Mg^{2+}]_i$ and $[Ca^{2+}]_i$ studied in isolated rat cardiomyocytes. *J Physiol* 496 (Pt 1): 111-128, 1996.

91. Li LZ, Zhou R, Zhong T, Moon L, Kim EJ, Qiao H, Pickup S, Hendrix MJ, Leeper D, Chance B and Glickson JD. Predicting melanoma metastatic potential by optical and magnetic resonance imaging. *Adv Exp Med Biol* 599: 67-78, 2007.

92. Li M and Yu X. The Role of Poly(ADP-ribosyl)ation in DNA Damage Response and Cancer Chemotherapy. *Oncogene* 34: 3349-3356, 2014.

93. Liimatta EV, Gödecke A, Schrader J and Hassinen IE. Regulation of cellular respiration in myoglobin-deficient mouse heart. *Mol Cell Biochem* 256-257: 201-208, 2004.

94. Lillig CH, Berndt C and Holmgren A. Glutaredoxin systems. *Biochim Biophys Acta* 1780: 1304-1317, 2008.

95. Lin SJ and Guarente L. Nicotinamide adenine dinucleotide, a metabolic regulator of transcription, longevity and disease. *Curr Opin Cell Biol* 15: 241-246, 2003.

96. Love NR, Pollak N, Dolle C, Niere M, Chen Y, Oliveri P, Amaya E, Patel S and Ziegler M. NAD kinase controls animal NADP biosynthesis and is modulated via evolutionarily divergent calmodulin-dependent mechanisms. *Proc Natl Acad Sci U S A* 112: 1386-1391, 2015.

97. Lu M, Zhu XH and Chen W. In vivo ^{31}P MRS assessment of intracellular NAD metabolites and NAD$^+$/NADH redox state in human brain at 4 T. *NMR Biomed* 29: 1010-1017, 2016.

98. Lukyanov KA and Belousov VV. Genetically encoded fluorescent redox sensors. *Biochim Biophys Acta* 1840: 745-756, 2014.

99. Lund FE. Signaling properties of CD38 in the mouse immune system: enzyme-dependent and -independent roles in immunity. *Mol Med* 12: 328-333, 2006.

100. Ma T, Peng Y, Huang W and Ding J. Molecular mechanism of the allosteric regulation of the alphagamma heterodimer of human NAD-dependent isocitrate dehydrogenase. *Sci Rep* 7: 40921, 2017.

101. Mailloux RJ. Teaching the fundamentals of electron transfer reactions in mitochondria and the production and detection of reactive oxygen species. *Redox Biol* 4: 381-398, 2015.

102. Marcu R, Wiczer BM, Neeley CK and Hawkins BJ. Mitochondrial matrix Ca^{2+} accumulation regulates cytosolic NAD$^+$/NADH metabolism, protein acetylation, and sirtuin expression. *Mol Cell Biol* 34: 2890-2902, 2014.

103. Marks AR, McIntyre JO, Duncan TM, Erdjument-Bromage H, Tempst P and Fleischer S. Molecular cloning and characterization of (R)-3-hydroxybutyrate dehydrogenase from human heart. *J Biol Chem* 267: 15459-15463, 1992.

104. Marsin AS, Bertrand L, Rider MH, Deprez J, Beauloye C, Vincent MF, Van den Berghe G, Carling D and Hue L. Phosphorylation and activation of heart PFK-2 by AMPK has a role in the stimulation of glycolysis during ischaemia. *Curr Biol* 10: 1247-1255, 2000.

105. Melo EP, Lopes C, Gollwitzer P, Lortz S, Lenzen S, Mehmeti I, Kaminski CF, Ron D and Avezov E. TriPer, an optical probe tuned to the endoplasmic reticulum tracks changes in luminal H_2O_2. *BMC Biol* 15: 24-017-0367-5, 2017.

106. Midgley PJ, Rutter GA, Thomas AP and Denton RM. Effects of Ca^{2+} and Mg^{2+} on the activity of pyruvate dehydrogenase phosphate phosphatase within toluene-permeabilized mitochondria. *Biochem J* 241: 371-377, 1987.

107. Mostoslavsky R, Chua KF, Lombard DB, Pang WW, Fischer MR, Gellon L, Liu P, Mostoslavsky G, Franco S, Murphy MM, Mills KD, Patel P, Hsu JT, Hong AL, Ford E, Cheng HL, Kennedy C, Nunez N, Bronson R, Frendewey D, Auerbach W, Valenzuela D, Karow M, Hottiger MO, Hursting S, Barrett JC, Guarente L, Mulligan R, Demple B, Yancopoulos GD and Alt FW. Genomic instability and aging-like phenotype in the absence of mammalian SIRT6. *Cell* 124: 315-329, 2006.

108. Mouchiroud L, Houtkooper RH, Moullan N, Katsyuba E, Ryu D, Canto C, Mottis A, Jo YS, Viswanathan M, Schoonjans K, Guarente L and Auwerx J. The NAD$^+$/Sirtuin pathway modulates longevity through activation of mitochondrial UPR and FOXO signaling. *Cell* 154: 430-441, 2013.

109. Mracek T, Holzerova E, Drahota Z, Kovarova N, Vrbacky M, Jesina P and Houstek J. ROS generation and multiple forms of mammalian mitochondrial glycerol-3-phosphate dehydrogenase. *Biochim Biophys Acta* 1837: 98-111, 2014.

110. Newman AC and Maddocks ODK. Serine and Functional Metabolites in Cancer. *Trends Cell Biol* 27: 645-657, 2017.

111. Nikiforov A, Dölle C, Niere M and Ziegler M. Pathways and subcellular compartmentation of NAD biosynthesis in human cells: From entry of extracellular precursors to mitochondrial NAD generation. *J Biol Chem* 286: 21767-21778, 2011.

112. Nogueira M, Garcia G, Mejuto C and Freire M. Regulation of the pentose phosphate cycle. Cofactor that controls the inhibition of glucose-6-phosphate dehydrogenase by NADPH in rat liver. *Biochem J* 239: 553-558, 1986.

113. Nuutinen EM. Subcellular origin of the surface fluorescence of reduced nicotinamide nucleotides in the isolated perfused rat heart. *Basic Res Cardiol* 79: 49-58, 1984.

114. Nuutinen EM, Hiltunen JK and Hassinen IE. The glutamate dehydrogenase system and the redox state of mitochondrial free nicotinamide adenine dinucleotide in myocardium. *FEBS Lett* 128: 356-360, 1981.

115. Ohashi K, Kawai S and Murata K. Identification and characterization of a human mitochondrial NAD kinase. *Nat Commun* 3: 1248, 2012.

116. Opie LH and Owen P. Effects of increased mechanical work by isolated perfused rat heart during production or uptake of ketone bodies. Assessment of mitochondrial oxidized to reduced free nicotinamide-adenine dinucleotide ratios and oxaloacetate concentrations. *Biochem J* 148: 403-415, 1975.

117. Orr AL, Quinlan CL, Perevoshchikova IV and Brand MD. A refined analysis of superoxide production by mitochondrial sn-glycerol 3-phosphate dehydrogenase. *J Biol Chem* 287: 42921-42935, 2012.

118. Oshino N, Jamieson D, Sugano T and Chance B. Optical measurement of the catalase-hydrogen peroxide intermediate (Compound I) in the liver of anaesthetized rats and its implication to hydrogen peroxide production in situ. *Biochem J* 146: 67-77, 1975.

119. Palmieri L, Pardo B, Lasorsa FM, del Arco A, Kobayashi K, Iijima M, Runswick MJ, Walker JE, Saheki T, Satrustegui J and Palmieri F. Citrin and aralar1 are Ca^{2+}-stimulated aspartate/glutamate transporters in mitochondria. *EMBO J* 20: 5060-5069, 2001.

120. Panday A, Sahoo MK, Osorio D and Batra S. NADPH oxidases: an overview from structure to innate immunity-associated pathologies. *Cell Mol Immunol* 12: 5-23, 2015.

121. Perl A, Hanczko R, Telarico T, Oaks Z and Landas S. Oxidative stress, inflammation and carcinogenesis are controlled through the pentose phosphate pathway by transaldolase. *Trends Mol Med* 17: 395-403, 2011.

122. Qi F, Chen X and Beard DA. Detailed kinetics and regulation of mammalian NAD-linked isocitrate dehydrogenase. *Biochim Biophys Acta* 1784: 1641-1651, 2008.

123. Ramos-Martinez JI. The regulation of the pentose phosphate pathway: Remember Krebs. *Arch Biochem Biophys* 614: 50-52, 2017.

124. Ratajczak J, Joffraud M, Trammell SA, Ras R, Canela N, Boutant M, Kulkarni SS, Rodrigues M, Redpath P, Migaud ME, Auwerx J, Yanes O, Brenner C and Canto C. NRK1 controls nicotinamide mononucleotide and nicotinamide riboside metabolism in mammalian cells. *Nat Commun* 7: 13103, 2016.

125. Ray Chaudhuri A and Nussenzweig A. The multifaceted roles of PARP1 in DNA repair and chromatin remodelling. *Nat Rev Mol Cell Biol*, 2017.

126. Rodgers JT, Lerin C, Haas W, Gygi SP, Spiegelman BM and Puigserver P. Nutrient control of glucose homeostasis through a complex of PGC-1alpha and SIRT1. *Nature* 434: 113-118, 2005.

127. Rodriguez-Segade S, Carrion A and Freire M. Isolation and purification of a regulating cofactor of the pentose-phosphate pathway. *Biochem Biophys Res Commun* 89: 148-154, 1979.

128. Rokka A, Antonenkov VD, Soininen R, Immonen HL, Pirila PL, Bergmann U, Sormunen RT, Weckstrom M, Benz R and Hiltunen JK. Pxmp2 is a channel-forming protein in mammalian peroxisomal membrane. *PLoS One* 4: e5090, 2009.

129. Satoh A, Brace CS, Rensing N, Cliften P, Wozniak DF, Herzog ED, Yamada KA and Imai S. Sirt1 extends life span and delays aging in mice through the regulation of Nk2 homeobox 1 in the DMH and LH. *Cell Metab* 18: 416-430, 2013.

130. Savolainen MJ and Hassinen IE. Mechanisms for the effects of ethanol on hepatic phosphatidate phosphohydrolase. *Biochem J* 176: 885-892, 1978.

131. Schlicker C, Gertz M, Papatheodorou P, Kachholz B, Becker CF and Steegborn C. Substrates and regulation mechanisms for the human mitochondrial sirtuins Sirt3 and Sirt5. *J Mol Biol* 382: 790-801, 2008.

132. Scholz R, Thurman RG, Williamson JR, Chance B and Bucher T. Flavin and pyridine nucleotide oxidation-reduction changes in perfused rat liver. I. Anoxia and subcellular localization of fluorescent flavoproteins. *J Biol Chem* 244: 2317-2324, 1969.

133. Schönfeld P and Wojtczak L. Brown adipose tissue mitochondria oxidizing fatty acids generate high levels of reactive oxygen species irrespective of the uncoupling protein-1 activity state. *Biochim Biophys Acta* 1817: 410-418, 2012.

134. Schueren F, Lingner T, George R, Hofhuis J, Dickel C, Gartner J and Thoms S. Peroxisomal lactate dehydrogenase is generated by translational readthrough in mammals. *Elife* 3: e03640, 2014.

135. Sekine N, Cirulli V, Regazzi R, Brown LJ, Gine E, Tamarit-Rodriguez J, Girotti M, Marie S, MacDonald MJ and Wollheim CB. Low lactate dehydrogenase and high mitochondrial glycerol phosphate dehydrogenase in pancreatic beta-cells. Potential role in nutrient sensing. *J Biol Chem* 269: 4895-4902, 1994.

136. Shi H, Enriquez A, Rapadas M, Martin EMMA, Wang R, Moreau J, Lim CK, Szot JO, Ip E, Hughes JN, Sugimoto K, Humphreys DT, McInerney-Leo AM, Leo PJ, Maghzal GJ, Halliday J, Smith J, Colley A, Mark PR, Collins F, Sillence DO, Winlaw DS, Ho JWK, Guillemin GJ, Brown MA, Kikuchi K, Thomas PQ, Stocker R, Giannoulatou E, Chapman G, Duncan EL, Sparrow DB and Dunwoodie SL. NAD deficiency, congenital malformations, and niacin supplementation. *N Engl J Med* 377: 544-552, 2017.

137. Sies H, Berndt C and Jones DP. Oxidative Stress. *Annu Rev Biochem* 86: 715-748, 2017.

138. Sies H and Chance B. The steady state level of catalase compound I in isolated hemoglobin-free perfused rat liver. *FEBS Lett* 11: 172-176, 1970.

139. Sies H, Häussinger D and Grosskopf M. Mitochondrial nicotinamide nucleotide systems: ammonium chloride responses and associated metabolic transitions in hemoglobin-free perfused rat liver. *Hoppe Seylers Z Physiol Chem* 355: 305-320, 1974.

140. Siess EA, Kientsch-Engel RI and Wieland OH. Concentration of free oxaloacetate in the mitochondrial compartment of isolated liver cells. *Biochem J* 218: 171-176, 1984.

141. Stein LR and Imai S. The dynamic regulation of NAD metabolism in mitochondria. *Trends Endocrinol Metab* 23: 420-428, 2012.

142. Stubbs M, Veech RL and Krebs HA. Control of the redox state of the nicotinamide-adenine dinucleotide couple in rat liver cytoplasm. *Biochem J* 126: 59-65, 1972.

143. Sugiura A, Mattie S, Prudent J and McBride HM. Newly born peroxisomes are a hybrid of mitochondrial and ER-derived pre-peroxisomes. *Nature* 542: 251-254, 2017.

144. Sundqvist KE, Heikkilä J, Hassinen IE and Hiltunen JK. Role of $NADP^+$-linked malic enzymes as regulators of the pool size of tricarboxylic acid-cycle intermediates in the perfused rat heart. *Biochem J* 243: 853-857, 1987.

145. Taylor EB. Functional properties of the mitochondrial carrier system. *Trends Cell Biol*, 2017.

146. Tedeschi PM, Markert EK, Gounder M, Lin H, Dvorzhinski D, Dolfi SC, Chan LL, Qiu J, DiPaola RS, Hirshfield KM, Boros LG, Bertino JR, Oltvai ZN and Vazquez A. Contribution of serine, folate and glycine metabolism to the ATP, NADPH and purine requirements of cancer cells. *Cell Death Dis* 4: e877, 2013.

147. Thomas DC. The phagocyte respiratory burst: Historical perspectives and and recent advances. *Immunol Lett*: https://doi.org/10.1016/j.imlet.2017.08.016 [Epub ahead of print], 2017.

148. Turner RS, Thomas RG, Craft S, van Dyck CH, Mintzer J, Reynolds BA, Brewer JB, Rissman RA, Raman R, Aisen PS and Alzheimer's Disease Cooperative Study. A randomized, double-

blind, placebo-controlled trial of resveratrol for Alzheimer disease. *Neurology* 85: 1383-1391, 2015.

149. Vachharajani VT, Liu T, Wang X, Hoth JJ, Yoza BK and McCall CE. Sirtuins link inflammation and metabolism. *J Immunol Res* 2016: 8167273, 2016.

150. van Roermund CW, Schroers MG, Wiese J, Facchinelli F, Kurz S, Wilkinson S, Charton L, Wanders RJ, Waterham HR, Weber AP and Link N. The peroxisomal NAD carrier from *Arabidopsis* imports NAD in exchange with AMP. *Plant Physiol* 171: 2127-2139, 2016.

151. VanLinden MR, Dolle C, Pettersen IK, Kulikova VA, Niere M, Agrimi G, Dyrstad SE, Palmieri F, Nikiforov AA, Tronstad KJ and Ziegler M. Subcellular distribution of NAD^+ between cytosol and mitochondria determines the metabolic profile of human cells. *J Biol Chem* 290: 27644-27659, 2015.

152. Varone A, Xylas J, Quinn KP, Pouli D, Sridharan G, McLaughlin-Drubin ME, Alonzo C, Lee K, Munger K and Georgakoudi I. Endogenous two-photon fluorescence imaging elucidates metabolic changes related to enhanced glycolysis and glutamine consumption in precancerous epithelial tissues. *Cancer Res* 74: 3067-3075, 2014.

153. Velick S. Fluorescence spectra and polarization of glyceraldehyde-3-phosphate and lactic dehydrogenase coenzyme complexes. *J Biol Chem* 233: 1455-1467, 1958.

154. Vielhaber S, Winkler K, Kirches E, Kunz D, Buchner M, Feistner H, Elger CE, Ludolph AC, Riepe MW and Kunz WS. Visualization of defective mitochondrial function in skeletal muscle fibers of patients with sporadic amyotrophic lateral sclerosis. *J Neurol Sci* 169: 133-139, 1999.

155. Vinogradov AD. $NADH/NAD^+$ interaction with NADH: ubiquinone oxidoreductase (complex I). *Biochim Biophys Acta* 1777: 729-734, 2008.

156. Waller JC, Dhanoa PK, Schumann U, Mullen RT and Snedden WA. Subcellular and tissue localization of NAD kinases from Arabidopsis: compartmentalization of de novo NADP biosynthesis. *Planta* 231: 305-317, 2010.

157. Wanders RJA, Waterham HR and Ferdinandusse S. Metabolic interplay between peroxisomes and other subcellular organelles including mitochondria and the endoplasmic reticulum. *Front Cell Dev Biol* 3: https://doi.org/10.3389/fcell.2015.00083, 2015.

158. Westerhoff HV and VanDam K. *Thermodynamics and control of biological free energy transduction*. Amsterdam: Elsevier, 1987.

159. Wikström M and Hummer G. Stoichiometry of proton translocation by respiratory complex I and its mechanistic implications. *Proc Natl Acad Sci U S A* 109: 4431-4436, 2012.

160. Williams PA, Harder JM, Foxworth NE, Cardozo BH, Cochran KE and John SWM. Nicotinamide and WLD^S act together to prevent neurodegeneration in glaucoma. *Front Neurosci* 11: 232, 2017.

161. Williamson JR and Cooper RH. Regulation of the citric acid cycle in mammalian systems. *FEBS Lett* 117 Suppl: K73-85, 1980.

162. Wilson DF. Oxidative phosphorylation: unique regulatory mechanism and role in metabolic homeostasis. *J Appl Physiol (1985)* 122: 611-619, 2017.

163. Wilson DF, Dutton PL, Erecinska M, Lindsay JG and Sato N. Mitochondrial electron transport and energy conservation. *Accounts Chem Res* 5: 234-241, 1972.

164. Wilson DF, Stubbs M, Veech RL, Erecinska M and Krebs HA. Equilibrium relations between the oxidation-reduction reactions and the adenosine triphosphate synthesis in suspensions of isolated liver cells. *Biochem J* 140: 57-64, 1974.

165. Xu HN, Nioka S, Chance B and Li LZ. Heterogeneity of mitochondrial redox state in premalignant pancreas in a PTEN null transgenic mouse model. *Adv Exp Med Biol* 701: 207-213, 2011.

166. Yeh TY, Sbodio JI, Tsun ZY, Luo B and Chi NW. Insulin-stimulated exocytosis of GLUT4 is enhanced by IRAP and its partner tankyrase. *Biochem J* 402: 279-290, 2007.

167. Yu Q and Heikal AA. Two-photon autofluorescence dynamics imaging reveals sensitivity of intracellular NADH concentration and conformation to cell physiology at the single-cell level. *J Photochem Photobiol B* 95: 46-57, 2009.

168. Zaha VG and Young LH. AMP-activated protein kinase regulation and biological actions in the heart. *Circ Res* 111: 800-814, 2012.

169. Zelewski M and Swierczynski J. Malic enzyme in human liver. Intracellular distribution, purification and properties of cytosolic isozyme. *Eur J Biochem* 201: 339-345, 1991.

170. Zhang H, Ryu D, Wu Y, Gariani K, Wang X, Luan P, D'Amico D, Ropelle ER, Lutolf MP, Aebersold R, Schoonjans K, Menzies KJ and Auwerx J. NAD^+ repletion improves mitochondrial and stem cell function and enhances life span in mice. *Science* 352: 1436-1443, 2016.

171. Zhang R. MNADK, a long-awaited human mitochondrion-localized NAD kinase. *J Cell Physiol* 230: 1697-1701, 2015.

172. Zhang R, Erler J and Langowski J. Histone acetylation regulates chromatin accessibility: Role of H4K16 in Inter-nucleosome Interaction. *Biophys J* 112: 450-459, 2017.

173. Zhong L, Yeh TY, Hao J, Pourtabatabaei N, Mahata SK, Shao J, Chessler SD and Chi NW. Nutritional energy stimulates NAD^+ production to promote tankyrase-mediated PARsylation in insulinoma cells. *PLoS One* 10: e0122948, 2015.

174. Zhu X, Lu M, Lee B, Ugurbil K and Chen W. In vivo NAD assay reveals the intracellular NAD contents and redox state in healthy human brain and their age dependences. *Proc Natl Acad Sci U S A* 112: 2876-2881, 2015.

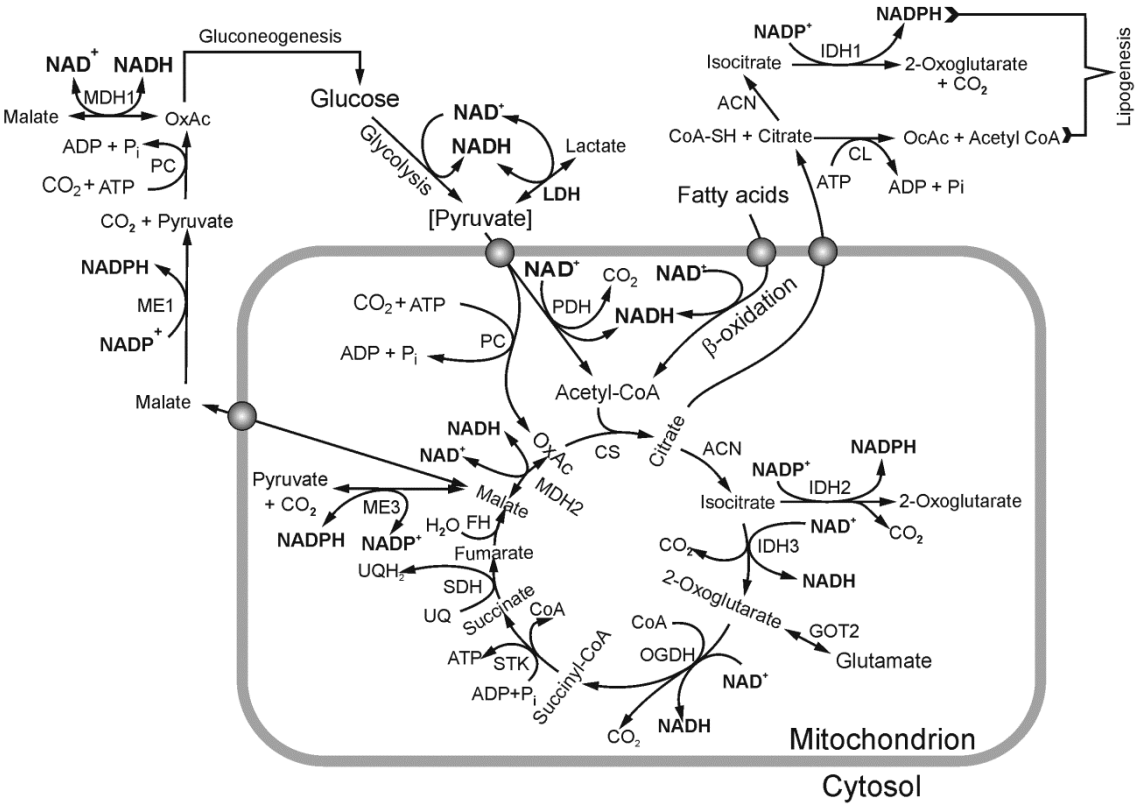

FIG. 1. Main NAD+- and NADP+-linked pathways of energy metabolism. Key enzymes of TCA cycle, gluconeogenesis, glycolysis, fatty acid oxidation and substrate provision for lipogenesis. CL, citrate lyase; PDH, pyruvate dehydrogenase complex; PC, pyruvate carboxylase; CS, citrate synthase; IDH1, cytosolic NADP-linked isocitrate dehydrogenase; IDH2, mitochondrial NADP-linked isocitrate dehydrogenase; IDH3, GOT2, mitochondrial aspartate transaminase; OGDH, 2-oxoglutarate dehydrogenase; STK, succinate thiokinase; SDH, succinate dehydrogenase; FH, fumarate hydratase; MDH1, cytosolic NAD-linked malate dehydrogenase; MDH2 mitochondrial NAD-linked malate dehydrogenase; ME1, cytosolic malic enzyme; ME3, mitochondrial malic enzyme.

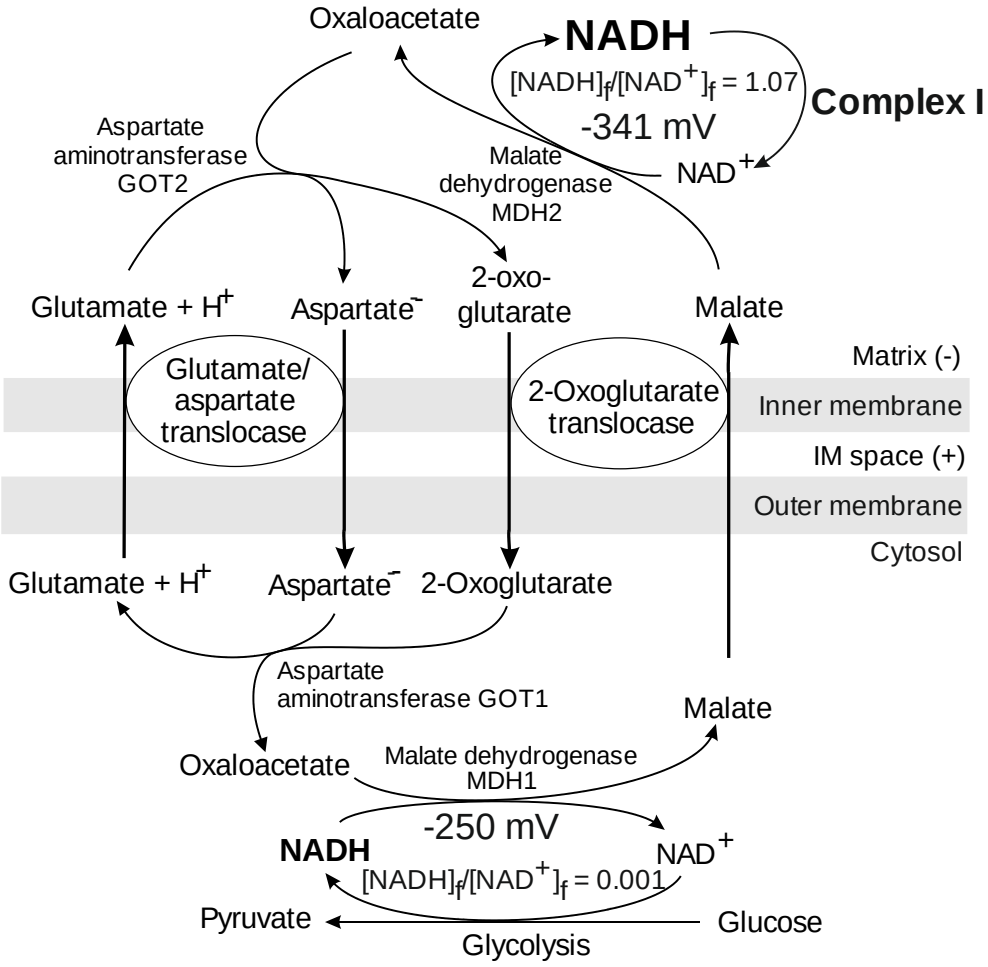

FIG. 2. Transfer of reducing equivalents from cytosolic NADH to the mitochondrial matrix against a redox gradient by the electrogenic malate-aspartate shuttle. The numerical values describing the redox poise in cytosol and mitochondrial matrix represent a metabolic situation in an isolated perfused rat heart (114).

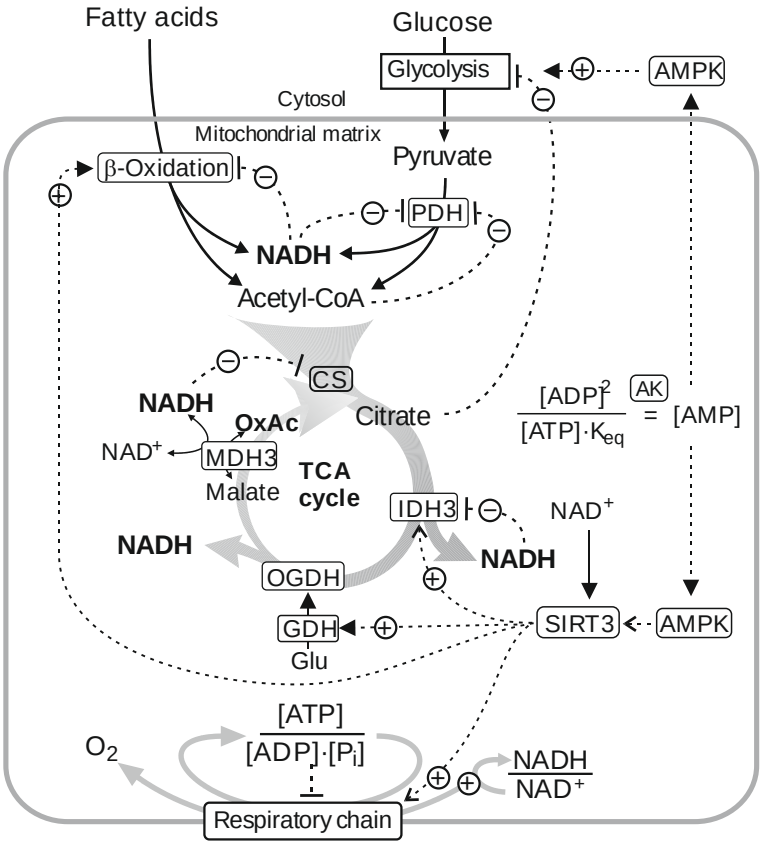

FIG .3. Redox potential- and energy-linked control of main catabolic pathways. The dashed arrows depict regulatory interactions. Mass-action equation of the adenylate kinase reaction is displayed to emphasize the amplification built in its $[ADP]^2$ term. AMPK, AMP-dependent protein kinase; GDH, glutamate dehydrogenase; OGDH, 2-oxoglutarate dehydrogenase; MDH3, NAD^+-linked malate dehydrogenase; IDH3, NAD^+-linked isocitrate dehydrogenase; CS, citrate synthase; PDH, pyruvate dehydrogenase complex; OxAc, oxaloacetate.

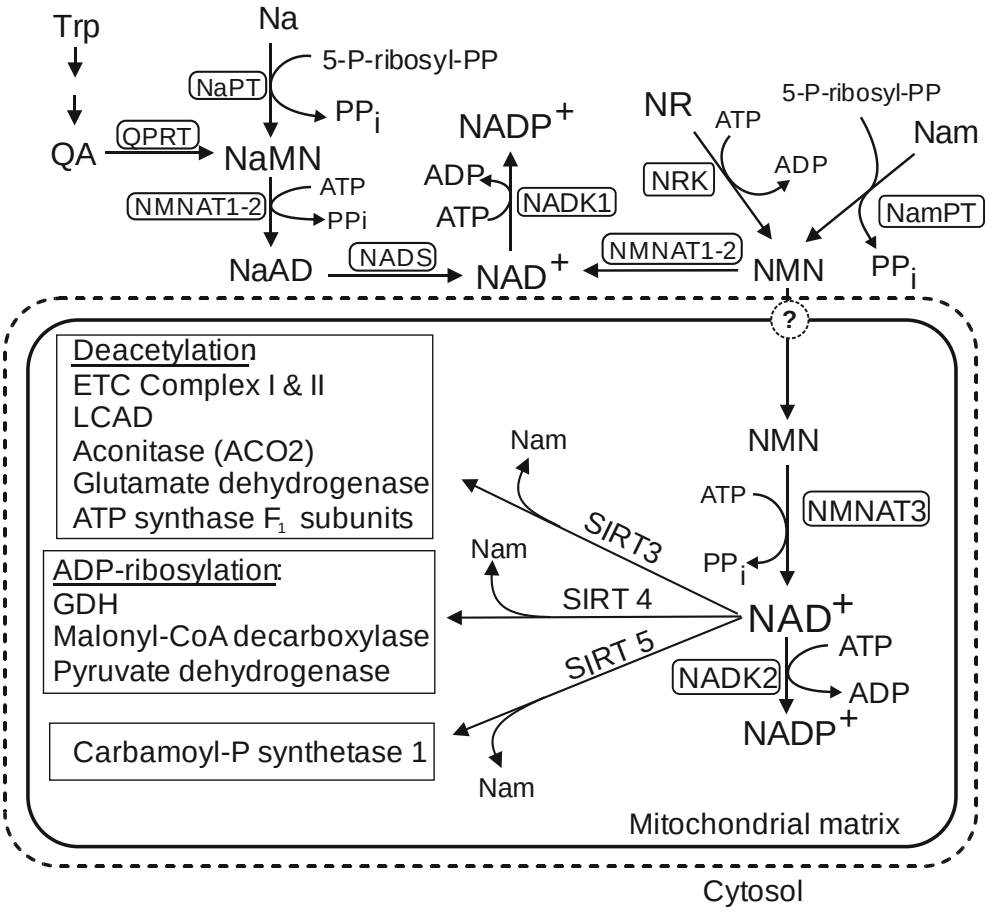

FIG. 4. NAD+ and NADP+ biosynthesis in cytosol, and consumption and salvage in mitochondria. Trp, tryptophan; QA, quinolinic acid; QPRT, quinolinate phophoribosyltransferase; Na, nicotinic acid; NaPT, nicotinic acid phosphoribosyltransferase; NMNAT, nicotinamide/nicotinic acid mononucleotide adenylyltransferase; NADS, NAD synthase; NaMN, nicotinic acid mononucleotide; Nam, nicotinamide; NamPT, nicotinamide phosphoribosyltransferase; NR, nicotinamide riboside; NRK, nicotinamide riboside kinase; NMAT1-2, nuclear and cytosolic nicotinamide mononucleotide adenylyltransferase isoforms 1 and 2; NMAT3, mitochondrial nicotinamide mononucleotide adenylyltransferase isoform 3; GDH, glutamate dehydrogenase; NADK1, cytosolic NAD kinase isoform; NADK2, mitochondrial NAD kinase isoform; ETC, electron transfer chain.

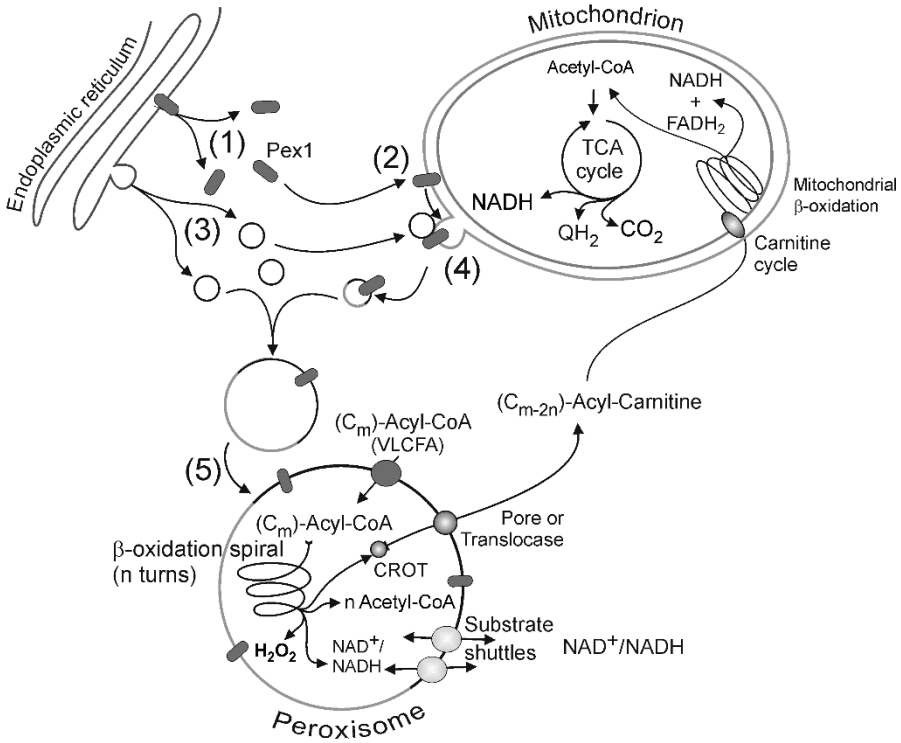

Fig. 5. Mitochondria and peroxisomes collaborate in both metabolism and biogenesis. (1) In the absence of peroxisomes the peroxins (peroxisomal assembly proteins) synthetized in the endoplasmic reticulum (2) are mistargeted to mitochondria. (3) *De novo* peroxisomes formed in the endoplasmic reticulum (4) make contact with the mitochondrial membrane to acquire peroxin (Pex1) and parts of mitochondrial membrane (mitochondrion-derived vesicles) (5) to obtain competence for maturation. Oxidation of very long-chain fatty acids (VLCFA, 22-28 carbon atoms) necessitates participation of peroxisomes because mitochondria are devoid of VLCFA CoA synthetase. Peroxisomal fatty acid oxidase system shortens the fatty acid molecule to a length acceptable by the mitochondrial acyl-CoA synthetase. CROT, carnitine octanoate transferase. For the redox substrate shuttle components, see Fig. 6.

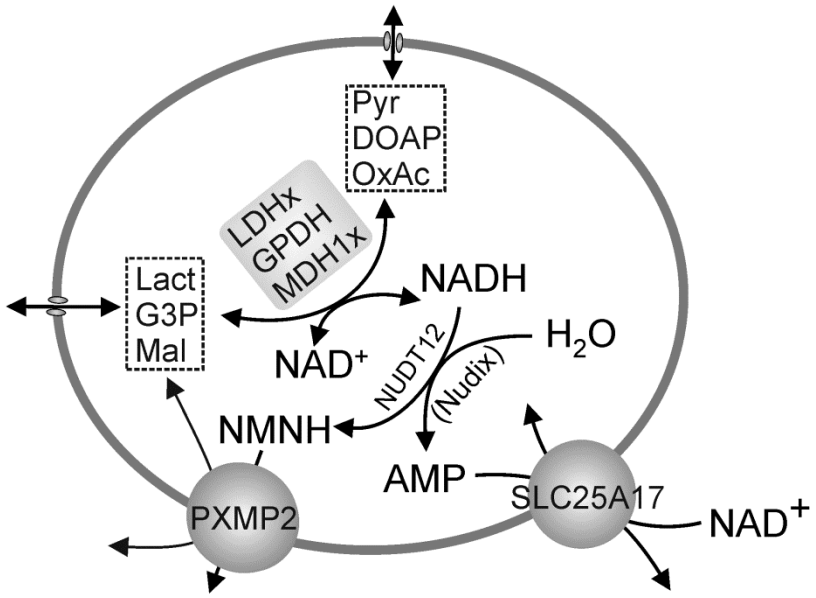

FIG. 6. Transmembrane traffic of reducing equivalents and pool size maintenance of NADH/NAD+ in peroxisomes. The membrane pores are permeable to small molecules so that some substrate shuttles operate without specific metabolite translocators. LDHx and MDH1x stand for translation read-through-extended forms of lactate and malate dehydrogenases, respectively. G3P, DOAP and GPDH stand for glycerol-3-phosphate, dihydroxyacetone phosphate and glycerol-3-phosphate dehydrogenase, respectively.